Journal of Sedimentary Research

Journal of Sedimentary Research, 2006, v. 76, 411–428
Research Article
DOI: 10.2110/jsr.2006.032

HOLOCENE DEPOSITIONAL HISTORY OF THE BURDEKIN RIVER DELTA OF NORTHEASTERN AUSTRALIA: A MODEL FOR A LOW-ACCOMMODATION, HIGHSTAND DELTA

CHRISTOPHER R. FIELDING,[1] JONATHON D. TRUEMAN,[2,3] AND JAN ALEXANDER[4]
[1]*Department of Geosciences, 214 Bessey Hall, University of Nebraska-Lincoln, Nebraska 68588-0340, U.S.A.*
[2]*Department of Earth Sciences, University of Queensland, Qld 4072, Australia*
[3]*BP Exploration Operating Company Ltd., Burnside Road, Farburn Industrial Estate, Dyce, Aberdeen AB21 7PB, U.K.*
[4]*School of Environmental Sciences, University of East Anglia, Norwich, NR4 7TJ, U.K.*
e-mail: cfielding2@unl.edu

ABSTRACT: **The Burdekin River of northeastern Australia has constructed a substantial delta during the Holocene (delta plain area 1260 km^2). The vertical succession through this delta comprises (1) a basal, coarse-grained transgressive lag overlying a continental omission surface, overlain by (2) a mud interval deposited as the coastal region was inundated by the postglacially rising sea, in turn overlain by (3) a generally sharp-based sand unit deposited principally in channel and mouth-bar environments with lesser volumes of floodplain and coastal facies. The Holocene Burdekin Delta was constructed as a series of at least thirteen discrete delta lobes, formed as the river avulsed. Each lobe consists of a composite sand body typically 5–8 m thick. The oldest lobes, formed during the latter stages of the postglacial sea-level rise (10–5.5 kyr BP), are larger than those formed during the highstand (5.5–3 kyr BP), which are in turn larger than those formed during the most recent slight sea-level lowering and stillstand (3–0 kyr BP). Radiocarbon ages and other stratigraphic data indicate that inter-avulsion period has decreased through time coincident with the decrease in delta lobe area. The primary control on Holocene delta architecture appears to have been a change from a pluvial climate known to characterize the region 12–4 kyr BP to the present drier, ENSO-dominated climate. In addition to decreasing the sediment supply via lower rates of chemical weathering, this change may have contributed to the shorter avulsion period by facilitating extreme variability of discharge. More frequent avulsion may also have been facilitated by the lengthening of the delta-plain channels as the system prograded seaward.**

INTRODUCTION

Most reviews of depositional models for deltaic systems (e.g., Galloway and Hobday 1996; Reading and Collinson 1996) emphasize those systems that issue into basins of substantial depth (tens to hundreds of meters). This emphasis probably derives from the focus of early research on deep-water systems such as the modern Mississippi, Rhone, and Niger deltas (see review by LeBlanc 1975) and the economic interest in analogous systems. Some recent classifications of deltas, however, explicitly allow for systems formed under conditions of more limited accommodation (e.g., Postma 1990, 1995). There are differences in facies character, distribution, and stacking patterns between deep-water deltas and their shallow-water equivalents.

Deltas that discharge onto shallow shelves tend to produce relatively thin vertical successions (typically a few meters thick). Rather than showing the coarsening-upward grain-size profile that many workers regard as typical of all deltas, the vertical successions of shallow-water deltas often comprise a lower fine-grained unit abruptly overlain by an upper, coarse-grained unit. This is true both of marine deltas (e.g., Colorado River, Kanes 1970; Guadalupe River, Donaldson et al. 1970; Brazos River, Rodriguez et al. 2000; Gilbert River, Jones et al. 2003) and their lacustrine counterparts (e.g., Atchafalaya Basin, Tye and Coleman 1989; Cumberland Marshes, Perez-Arlucea and Smith 1999; Farrell 2001; Volga River, Overeem et al. 2003; Lake Eyre, Lang et al. 2004).

In shallow receiving basins, river-mouth processes are typically dominated by bed friction, resulting in the deposition of elongate mouth-bar and delta-front sands. An example of this is the Volga River delta, which, because of the very low gradient, maintains frictional effluent conditions out onto the delta front (Overeem et al. 2003). Most marine deltas show some evidence of sediment reworking by tides and waves at the river mouth, producing a greater variety of mouth-bar geometries. Exceptions to this are bayhead deltas that are protected by coastal or offshore barriers (e.g., Guadalupe Delta, Donaldson et al. 1970). In general, mouth-bar and associated sands (beaches, etc.) in open shallow marine deltas tend to be more extensive than those of lacustrine deltas or protected marine deltas, either in the dip direction in the case of tide-influenced deltas or strike-elongate in the case of wave-influenced deltas (e.g., Jones et al. 2003; Kanes 1970; Rodriguez et al. 2000). The common factor among these examples, however, is that frictional attenuation of outflow dominates depositional processes at the river mouth (Wright 1977), producing potentially sharp-based mouth bar to delta front sand bodies.

The Burdekin River delta of northeastern Australia is one of the largest deltas in Australia, the river discharging onto the Great Barrier Reef shelf of the Coral Sea (Hopley 1970; Coleman and Wright 1975; Belperio 1983; Fielding et al. 2005a). The Holocene delta platform is made up of a number of sharp-based, medium- to coarse-grained sand bodies of

 1527-1404/06/076-411/$03.00

channel and mouth-bar origin deposited predominantly during short-duration, high-river-discharge events, and on this basis Fielding et al. (2005a, 2005b) proposed that the delta should be regarded as flood-dominated (i.e., constructed principally during major river outflow events), with some wave influence and minor tidal influence. Drill-hole and radiocarbon age data indicate that the Holocene succession is < 25 m thick over much of the delta, approximately equivalent to the depth of water into which the modern delta is prograding (Fielding et al. 2005a, 2005b).

The Holocene succession overlies a pronounced discontinuity surface that is readily picked from seismic reflection data (Reflector "A;" Orme et al. 1978). On land, where this interface has been intersected by drilling, it corresponds to an abrupt downward change from unconsolidated sediments to stiff, consolidated, generally reddened sands and clays with rhizocretions and pedogenic carbonate nodules. Radiocarbon ages from pedogenic carbonate within the substrate indicate that it is Pleistocene (Table 1). The Holocene interval therefore, can be regarded as a "sequence" in the genetic sense, bounded at the base by a sequence boundary formed during the last glacial sea-level lowstand. This paper documents the facies distribution and stratigraphic stacking patterns of the Holocene Burdekin Delta sequence and interprets these in the context of the regional sea-level history (Larcombe et al. 1995). How the interplay of sea-level rise, changing climate, and sediment dispersal patterns influence the architecture of the delta is examined. The delta is interpreted to comprise at least thirteen discrete delta lobes, exploiting the available, limited accommodation space afforded by the highstand Great Barrier Reef shelf, and we suggest that the resulting model of stratigraphic architecture might be applicable to other river deltas formed in circumstances controlled by limited accommodation.

THE BURDEKIN RIVER DELTA

A brief introduction to the Burdekin River delta is provided here. For more detailed information refer to Fielding et al. (2005a, 2005b). The Burdekin River has the largest discharge of any northeastern Australian drainage to the Coral Sea, and has a drainage basin area of 129,500 km^2 (Fig. 1; Neil et al. 2002). Although the headwaters of the trunk stream are in highlands covered by humid tropical rainforest, much of the drainage basin comprises sparsely vegetated lowlands and plains that receive a mean annual rainfall of 500–700 mm. Consequently, mean annual water and sediment discharge are modest (estimates range from 2.7×10^6 to 9.0×10^6 metric tons for sediment) compared to perennial streams of comparable size (Belperio 1983; Neil et al. 2002). The distribution of precipitation is strongly seasonal and variable from year to year, being controlled mainly by the erratic passage of tropical cyclones and development of monsoon troughs. Intense rainfall gives rise to rapid runoff and causes short-duration, high-magnitude fluvial discharge events mostly occurring between January and April (Alexander et al. 1999; Amos et al. 2004). These events, each of which might last from one to several days, deliver most of the annual sediment discharge to the delta (Belperio 1978; Alexander et al. 1999; Amos et al. 2004).

The Burdekin River has constructed a broad delta plain during the Quaternary (total area 1260 km^2; Fig. 1). At present, the southern part of the delta (c. 872 km^2) is "active" with coastline maintenance resulting from continued sediment supply by the river. The northern part of the delta plain appears largely inactive, in that it is not currently receiving significant fluvial sediment, and it has a quite different geomorphic character (Fielding et al. 2005a). Both active and inactive portions of the delta plain are crossed by numerous paleochannel courses that bifurcate as they approach the coast in the manner of deltaic distributaries (Fig. 1). This pattern suggests that sediment dispersal has been distributed across the broadly fan-shaped delta plain in a series of discrete areas through the most recent past.

The modern Burdekin River discharges onto the central Great Barrier Reef shelf or lagoon in an area that is partly protected from ocean swell by the large coastal bedrock headland of Cape Upstart (Fig. 1). The northern (abandoned) coast of the delta is also protected by a 14-km-long, recurved sand spit (Cape Bowling Green; Fig. 1). The delta coastline is strongly affected by waves driven by the prevailing southeasterly trade winds, which approach the coast obliquely, and is also strongly affected by summer tropical cyclones. The prevailing fair-weather winds and associated waves maintain a well-mixed, turbid water column most of the year and are also responsible for a strong northwestward (shore-parallel) current on the shoreface and inner shelf (Orpin et al. 1999; Larcombe and Carter 2004). Cyclones, which affect the area every 1–2 years, generate strong winds of variable direction, rough seas, and storm surges up to 3 m high. Given that sediment resuspension by wave activity seldom occurs on the inner shelf in water depths greater than 15 m, but that during the passage of tropical cyclones resuspension may occur in middle shelf water depths (20–35 m), fair-weather wave base is regarded as c. 15 m and storm wave base as c. 35 m (Orpin 1999; Orpin et al. 1999). The tidal regime on the Burdekin Delta is mesotidal (mean tidal range c. 2.5 m), semidiurnal, and asymmetrical. Orpin et al. (1999) contend that wind-driven waves and currents, and to a lesser extent tidal currents, are the dominant processes on the Great Barrier Reef shelf, whereas Larcombe and Carter (2004) contend that tropical cyclones exert the principal control on sediment dispersal.

METHODS

Surface geomorphology and sediment distribution were assessed on land by direct observation and sampling, using a hand auger and vibracorer, combined with remotely sensed imagery (e.g., Harvey 1998; Trueman 2002; Alexander and Fielding 2006) and by reference to the work of Hopley (1970) and Belperio (1978, 1983). Suspension and bed load were measured in the main channel in 2000 (Amos et al. 2004), and samples from the bed in successive dry seasons have been analyzed. A boat was used to take sediment grab samples in the lower distributary channels and on newly forming mouth bars during low flow conditions in March 2001, and fifteen samples were collected from largely abandoned distributaries and tidal channels over the period 1998–2001. We utilized an existing subsurface database from irrigation drilling undertaken mostly on the upper delta plain by the Irrigation and Water Supply Commission (IWSC; now administered by the Queensland Department of Natural Resources and Mines), and we undertook an extensive drilling campaign focusing on the lower delta plain. Twenty-four holes were drilled to a maximum of 18 m using a JACRO 350 trailer-mounted rig with 0.15 m diameter, hollow-stem auger rods. Sediment samples were taken from selected borehole intervals. Subsurface stratigraphy was also examined in all available cutbank and other exposures, and by ground-penetrating radar (GPR) traverses across selected sites using a Malå Geosciences RAMAC/GPR unit with 100 and 200 MHz antennas. Most samples were dry-sieved after removing the coarser gravel fraction (which was measured by calipers). Muddy samples were wet-sieved, and the fine fraction was analyzed with a laser particle sizer, and coarse fraction was dry-sieved. Geochronological data (Table 1) were acquired by the radiocarbon method on samples of mollusk shell or woody organic matter (found in growth position, wherever possible) and corrected for the marine reservoir effect where appropriate (Gillespie and Polach 1979). Caution was exercised in using radiocarbon ages, because some suites of ages from within individual drillholes displayed internal inconsistency, suggesting local reworking of organic material.

The broad pattern of surface sediment distribution in the subaqueous part of the delta has been established by previous work (Belperio 1978, 1983; Way 1987; Orpin 1999; Orpin et al. 2004). Limited data are available on the subsurface sediment distribution offshore from

TABLE 1.—*Radiocarbon ages from the Burdekin River Delta region, both from this study and from previous studies.*

Sample	Age (yr BP)	Error (±)	Easting	Northing	What dated?	Description
1. Radiocarbon Ages from this study						
ALV016	560	60	549978.77	7850656	Fleshy wood	Mud exposed on beach north of Alva
ALV017	1250	80	549978.77	7850656	Shell layer	Mud exposed on beach, north of Alva
CBG003	1010	80	547636.73	7858224	Wood	Mud exposed on beach, Cape Bowling Green
GIN003	830	60	562202	7816056	Shells	Dune ridge near Beach Mount
INK007	320	40	539630	7819369	Wood debris	from 0.5–0.6 m in INK-A2, southwest of Home Hill
INK010	8130	190	558116	7817501	Shells	from 8.0–9.7 m in INK-D1, Wallaces Landing
INK011	7350	50	558116	7817501	Wood debris	from 8.0–8.7 m in INK-D1, Wallaces Landing
PLA003	890	50	553500	7840500	Shells	from top of parabolic dune, Plantation Creek Landing
PLA005	1930	50	553745	7839950	Detrital wood	from 3.8–4.0 m in PLA-D1, Plantation Creek Landing
PLA006	2040	40	553745	7839950	Shells	from 4–6 m in PLA-D1, Plantation Creek Landing
PLA007	2280	100	553745	7839950	Wood fragments	from 4–6 m in PLA-D1, Plantation Creek Landing
PLA009	3330	50	553745	7839950	Wood	from 9.0–9.6 m in PLA-D1, Plantation Creek Landing
RIT010	190	70	560350	7826550	Charcoal	bank exposure of beach ridge facies, Rita Island south edge
RIT011	970	70	559095	7826274	Shell	bank exposure of beach ridge facies, Rita Island south edge
RIT012	1670	60	556011	7827408	Charcoal	from 3.6 m in RIT-D1, Rita Island
RIT015	3240	50	556011	7827408	Shell	from 7.5 m in RIT-D1, Rita Island
UPS100	6560	40	574742	7817125	Single bivalve shell	from 1.4 m in JCU marine vibrocore 853-VC2, Upstart Bay
INK100A	3460	90	557414	7820387	shells	from deflating dune ridge south of Groper Creek
RIT100	370	60	559004	7826318	mangrove roots	bank exposure of mangrove flat facies, Rita Island south edge
RIT101	670	60	556100	7825700	shells	bank exposure of beach ridge facies, Rita Island south edge
RIT103	350	50	560197	7828493	shells	from deflating eolian dunes (Set 3), Rita Island
RIT104	560	60	557714	7827555	shells	from deflating eolian dunes (Set 2), Rita Island
RIT108	4040	40	557714	7827555	shells	from 10.5 m in RIT-D2, Rita Island
RIT110	2040	40	557249	7826758	shells	from 3.6–4.4 m in RIT-D3, Rita Island
RIT112	1860	40	557249	7826758	shells	from 9.0 m in RIT-D3, Rita Island
RIT115	1110	40	556856	7826174	mangrove roots/ wood	from 3.0 m in RIT-D4, Rita Island
RIT117	1680	40	556856	7826174	shells	from 9.0 m in RIT-D4, Rita Island
RIT121	4490	60	555190	7827456	carbonised wood	from 8–10 m in RIT-D5, Rita Island
RIT123	3900	100	555190	7827456	shells	from 9.0 m in RIT-D5, Rita Island
ALV101	460	40	549673	7850477	wood fragments	from 1.65 m in ALV-D1, Lynch's Beach, Alva
ALV107	1340	40	549673	7850477	shell	single bivalve from 3.9 m in ALV D-1, Lynch's Beach, Alva
ALV108	1920	80	549673	7850477	shell fragments	from 5.6 m in ALV-D1, Lynch's Beach, Alva
ALV110	4330	50	549673	7850477	charcoal fragments	from 10.35 m in ALV-D1, Lynch's Beach, Alva
ALV112	30	90	552131	7847258	wood fragments	from north shore of tidal inlet in Alva spit
ALV207	3000	40	550500	7848000	shells	from 11.3–12.0 m in ALV-D2, south side of Alva
ANA302	100	?	559982	7831887	wood fragments	from channel floor of tidal inlet, mouth of Anabranch
GAI205	4640	90	544315	7849399	shells	from 12.0–13.1 m in GAI-D1, Gainsford station
GAI206	5220	50	544315	7849399	shells	from 13.1–13.5 m in GAI-D1, Gainsford Station
GAI217	111	?	544611	7849558	mangrove roots	from 1.1–1,2 m in GAI-V2
HUC202	4020	40	526030	7850000	wood fragments	from 7.2 m in HUC-D1, Huck's Landing
HUC203	6810	40	526030	7850000	shells	from 8.3–8.7 m in HUC-D1, Huck's Landing
MUD201	3140	50	552384	7841711	wood fragments	from 5.4–5.5 m in MUD-D1, Ocean Creek Landing
MUD203	5230	40	552384	7841711	shells	from 12.0–13.5 m in MUD-D1, Ocean Creek Landing
RIT201	2140	130	556370	7825655	charcoal	from deflating eolian dunes (Set 1), Rita Island
RIT202	2990	70	556437	7825708	shells	from mangrove mud at low water mark, Rita Island south edge
RIT211	1430	40	559078	7830188	charcoal	from 7.2–7.5 m in RIT-D6, Hell Hole Creek Landing
RIT215	3160	40	559078	7830188	shells	from 14.0–15.2 m in RIT-D6, Hell Hole Creek Landing
RIT223	360	40	560630	7828594	shells	from 1.93–2.04 m in RIT-V2, ocean beach, southeast Rita Island
2. Radiocarbon Ages from Previous Studies						
AW1*	1190	80	551400	7848400	plant detritus	Alva Beach (position approximate): Way, 1987
AW2	400	90	572470	7816765	*Kereia*	Vibrocore 853-VC3, Upstart Bay, at 0.46 m BSF (uncompacted): Way, 1987
AW3	4760	190	572470	7816765	*Ostrea bresia*	Vibrocore 853-VC3, Upstart Bay, at 2.00 m BSF (uncompacted): Way, 1987
AW4	5171	310	571959	7819903	micromolluscs	Vibrocore 853-VC9, Upstart Bay, at 3.26 m BSF (uncompacted): Way, 1987
GaK 2009*	480	80	558000	7826300	shell	"Deltaics" from south edge, Rita Island, seaward of dune: Hopley, 1970

TABLE 1.—*Continued.*

2. Radiocarbon Ages from Previous Studies

Sample	Age (yr BP)	Error (±)	Easting	Northing	What dated?	Description
GaK 2011*	25150	1050	552000	7815000	calcarenite cement	Dune ridge south of Mt Inkerman: Hopley, 1970
Coleman*	26900	900	554000	7813000	cemented shells	Beach rock from ridge south of Mt Inkerman: Hopley, 1970
GaK 2012*	3680	90	564000	7813500	mangrove root stump	Coast south of Sugar Loaf hill, below modern/ancient dunes: Hopley, 1970
GaK 2013*	750	80	588500	7810000	shell	Midden from outer barrier, Cape Upstart: Hopley, 1970
GaK 2415*	3200	110	556200	7825750	mangrove peat	South edge, Rita Island, beneath beach ridge: Hopley, 1970
GaK 2429*	28900	2800	552000	7815000	calcarenite cement	Check date on GaK 2011: Hopley, 1970
GaK 2431*	7530	180	587500	7808000	shell	White sands of double barrier system, Cape Upstart: Hopley, 1970
GaK 2430*	0	100	554000	7812000	shell	Yellow Gin Creek, behind "Pleistocene" ridge: Hopley, 1970
GaK 2998*	3830	120	525000	7850000	shell	Mangrove mud 8.5 ft below surface near estuary, Barratta Ck: Hopley, 1972
GaK 2999*	330	80	512000	7854000	wood	Channel deposits near mouth of Haughton River: Hopley, 1972
GaK 3000*	0	310	557000	7834000	shell	Phillips Landing bore (+2.9 m above MHWS), 22 ft below surface: Hopley, 1972
GaK 3001*	2240	200	557000	7834000	mangrove mud	Phillips Landing bore (+2.9 m above MHWS), 10 ft below surface: Hopley, 1972
GaK 3002	4700	140	557000	7834000	carbonate nodules	Phillips Landing bore (+2.9 m above MHWS), 44 ft below surface: Hopley, 1972
GaK 3003*	1000	100	557000	7834000	shell	Phillips Landing bore (+2.9 m above MHWS), 44–48 ft below surface: Hopley, 1972
GaK 3004*	240	380	557000	7834000	shell	Phillips Landing bore (+2.9 m above MHWS), 50 ft below surface: Hopley, 1972
GaK 3005*	1230	100	551400	7848400	shell	Alva Beach bore (+18 ft above MHWS), 22 ft below surface: Hopley, 1972
GaK 3006*	720	430	551400	7848400	mangrove wood	Alva Beach bore (+18 ft above MHWS), 20 ft below surface: Hopley, 1972
GaK 3007*	2180	100	551400	7848400	shell	Alva Beach bore (+18 ft above MHWS), 38 ft below surface: Hopley, 1972
GaK 3008*	2290	110	551400	7848400	shell	Alva Beach bore (+18 ft above MHWS), 50 ft below surface: Hopley, 1972
GaK 3009*	15100	400	551400	7848400	carbonate nodules	Alva Beach bore (+18 ft above MHWS), 78 ft below surface: Hopley, 1972
GaK6014	2200	200	533256	7858563	wood fragment	Bowling Green Bay, core 6.5 cm below sea floor: Belperio, 1978
GaK 6016	4970	170	547946	7842792	shell	Alva Beach road bore at 11 m below surface (−5 m R.L.): Belperio, 1978
GaK 6017	27350	?	518477	7841310	fresh water peat	IWSC water bore B6, Giru, at 20 m below surface (+4 m R.L.): Belperio, 1983
GaK 6721	330	70	547227	7846544	*Telescopium*	surface of deflating chenier beach ridge: Belperio, 1978
GaK 6722	350	80	548989	7851150	*Telescopium*	surface of deflating chenier beach ridge: Belperio, 1978
GaK 6723	3000	350	548989	7851150	organic-rich sand	deflating chenier beach ridge, 2.0 m depth below surface (+1.5 m R.L.): Belperio, 1978
I-1888*	2060	115	549400	7853000	mangrove mud	base of Cape Bowling Green: Thom et al., 1969
Coleman 1*	2060	115	550500	7849000	wood from peat	"peat" exposed at low tide, Alva Beach: Hopley, 1970
Coleman 2*	3460	110	513000	7854000	shell	mouth of Haughton River: Hopley, 1970
no ID*	3870	50	550500	7849000	carbonised wood	from low cliff above beach at Alva: Paine et al., 1966
UB1*	6730	30	566000	7812000	wood	Upstart Bay beach: Larcombe et al., 1995
no ID*	28900	1700	unknown	unknown	shell	"A Burdekin Delta Shoreline": Hopley & Murtha, 1975
no ID*	26900	900	unknown	unknown	shell	"A Burdekin Delta Shoreline": Hopley & Murtha, 1975
no ID*	25150	1050	unknown	unknown	carbonate cement	"A Burdekin Delta Shoreline": Hopley, 1970

Dates are reported as conventional ages in radiocarbon years BP, corrected where appropriate for the marine reservoir effect (Gillespie and Polach 1979) and with one standard deviation error. * denotes approximate locations. BSF = below sea floor. MHWS = maximum high water stage.

vibracores (Belperio 1978, 1983; Way 1987; Orpin 1999). Several hundred line kilometers of new seismic reflection data across the delta front and inner shelf were acquired using a Datasonics CAP-6600 CHIRP II acquisition and processing system deployed from the vessel RV James Kirby (Fielding et al. 2003; Fielding et al. 2005a; Fielding et al. 2005c).

GEOMORPHOLOGY, LITHOFACIES, AND HOLOCENE STRATIGRAPHY

The present-day Delta Plain can be divided on the basis of geomorphic criteria into an Upper Delta Plain that is unaffected by marine processes and characterized by fresh groundwater conditions, and a Lower Delta Plain that is affected by marine currents and waves, and in which

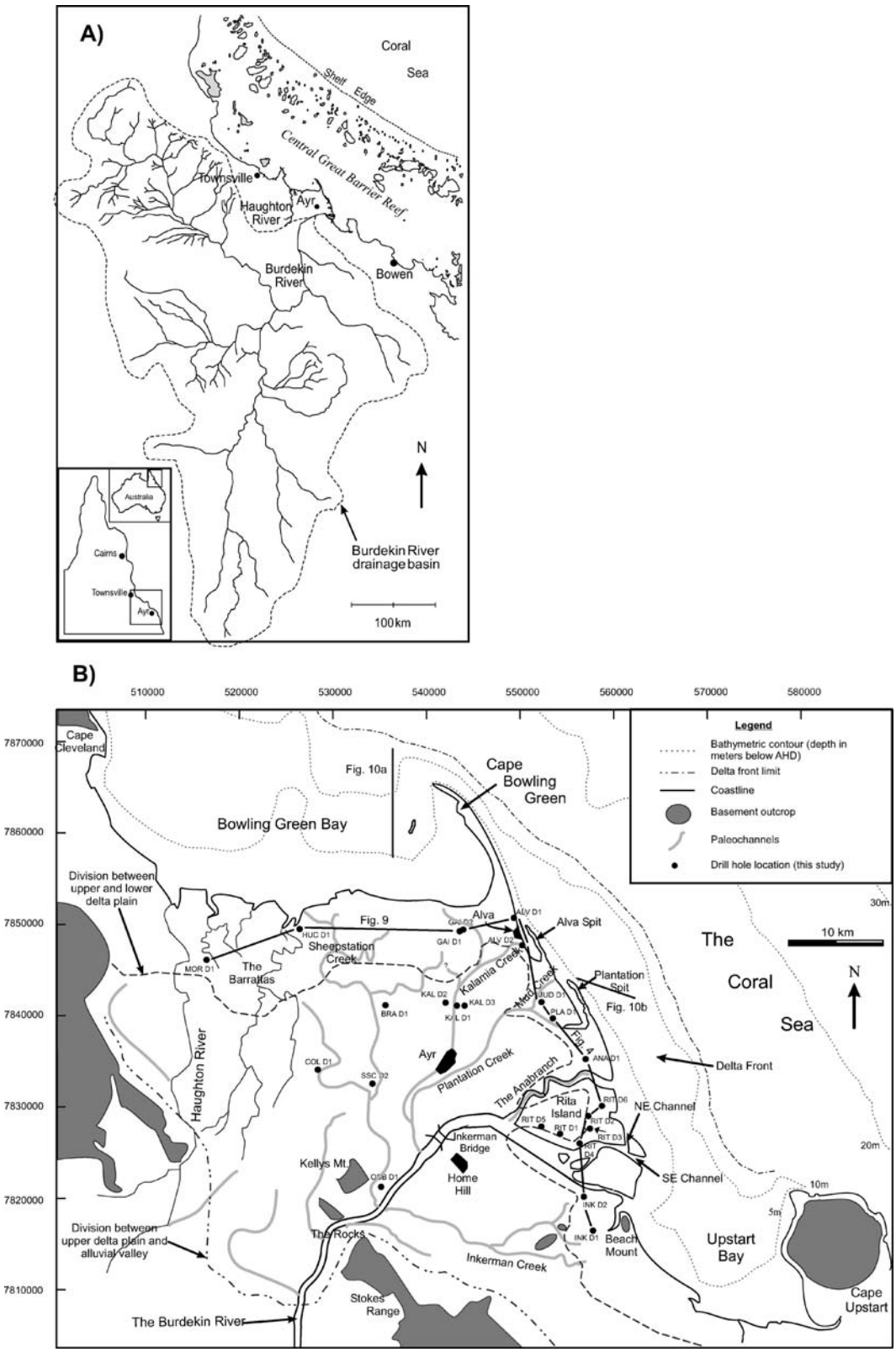

FIG. 1.—Maps showing the location of the Burdekin River drainage basin and delta in northeastern Australia, and of the delta plain, showing the location of major geomorphic boundaries, channels and paleochannels, and holes drilled during this study.

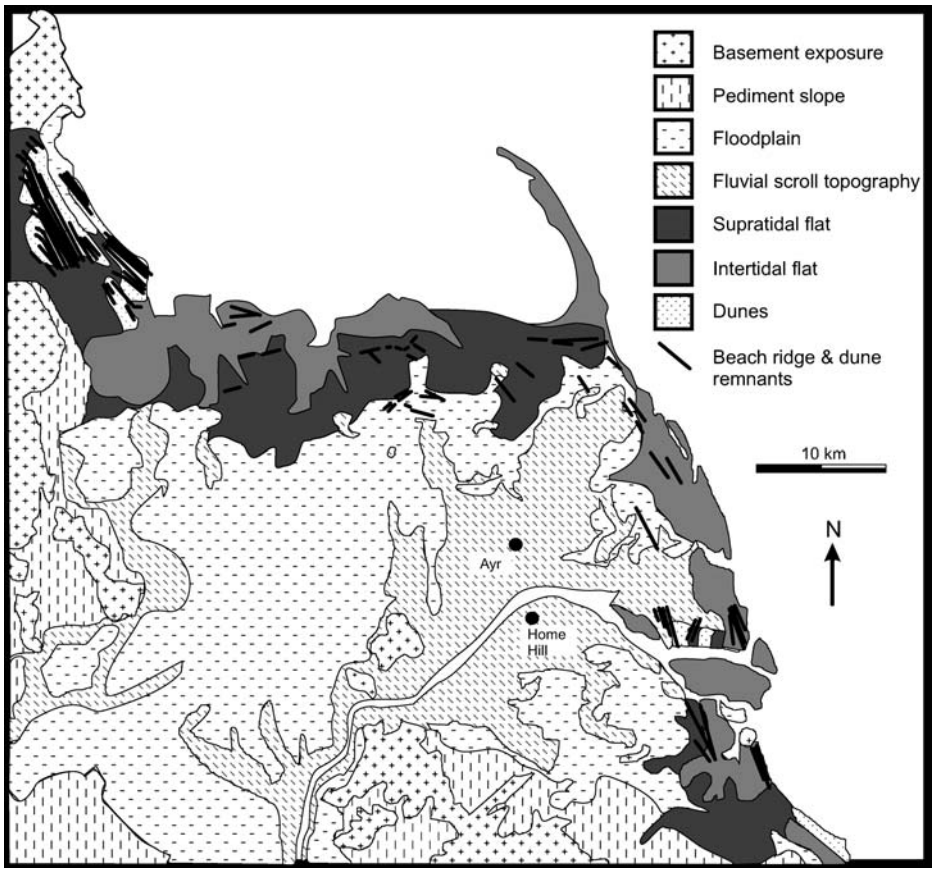

FIG. 2.—Geomorphology of the Burdekin River delta. Note the distribution of linear beach-ridge and foredune complexes, which denote former positions of the shoreline. The boundary between the Lower and Upper Delta Plain corresponds to the change from deep gray tones to lighter shades on the map.

brackish groundwater conditions prevail (Figs. 1, 2). A complete description of the depositional environments and lithofacies is presented by Fielding et al. (2005a), but a brief description is given here to allow the reader to evaluate subsequent stratigraphic interpretations.

The Upper Delta Plain is largely covered by scroll topography of abandoned distributary channels, active and abandoned channel courses, and floodplains (Fig. 2, Table 2), and is now intensely cultivated. Numerous channels and abandoned channels are preserved on the modern Delta Plain (Fig. 1), indicating that the route of sediment dispersal has moved across the delta from time to time during the Holocene. Beneath the veneer of (anthropogenically modified) topsoil, much of the Upper Delta Plain is covered by medium- to very coarse-grained, gravelly sand, suggesting that both channel and floodplain facies are dominantly sand (Table 1). This impression is confirmed by drilling data, which show stacked, erosionally based sand bodies in the subsurface throughout the Upper Delta Plain (Fig. 3, and see Alexander and Fielding 2006).

The Lower Delta Plain is a more complex mosaic of depositional environments or geomorphic elements (Fig. 2, Table 2). The coarsest-grained facies are distributary-channel and mouth-bar sands and gravelly sands (Table 2). Distributary-channel sands are indistinguishable texturally from Upper Delta Plain sands (Fielding et al. 2005a) but are typically coarser grained than any other facies on the delta and contain plant debris and minor shell fragments. Mouth-bar sands tend to be a little finer grained, lacking gravel, and contain dispersed pumice, plant fragments, and more abundant shell material. Both form sharp-based sand bodies 5–8 m thick (Fielding et al. 2005b). Deposits of tidal creeks may also include coarse-grained sands (introduced by flood runoff) with shell and plant debris, but they typically contain a component of mud, dispersed within sand and/or as discrete partings (Table 2; Fielding et al. 2005a, 2005b). Foreshores, beach ridges, and eolian dunes are represented by well-sorted, fine- to medium-grained sands that are distinctively different from channel and mouth-bar facies, but are often not easily distinguished from each other in the subsurface. Spits accumulate sands which have similar textural characteristics and which are indistinguishable from foreshore deposits in the subsurface (Fielding et al. 2005a). A variety of linear remnants of paleo-shoreline ridges are preserved on the present Lower Delta Plain and are interpreted to record former positions of the shoreline (Fig. 2). Various types of coastal flats are well represented on the modern Lower Delta Plain surface. The deposits of these flats are mainly muds, with some interlayered sand, and in some cases evaporites and biolaminations. Their grain size thus distinguishes them from other facies, but additionally the abundance of invertebrate shells of known coastal flat affinities, and of the roots of mangroves and other halophytic vegetation, makes it easy to identify these facies (Table 2; Fielding et al. 2005a). Marine muds are also encountered in the subsurface, and, from the distribution of such mud in the modern nearshore marine environment, are interpreted to record distal delta front to open marine bay environments.

The Holocene succession (Fig. 4) shows certain consistent patterns of facies stacking. The Holocene interval is generally < 25 m thick over much of the active delta coast (Fig. 5), and typically comprises (1) a basal lag of sand and gravel, often rich in invertebrate shells, overlain by (2) a mud-dominated section, which is in turn overlain either gradationally or (more commonly) sharply by (3) a sand-dominated section (Fig. 4). A significant portion of the upper sand-dominated section in most of our drillholes is composed of distributary-channel and mouth-bar deposits, and we therefore propose that the Holocene delta has been constructed principally via the progradation of new mouth bars and associated feeder

TABLE 2.—*Depositional environments of the Burdekin River delta and corresponding lithofacies.*

Environmental Setting	Characteristic Lithofacies
Upper Delta Plain	
Channel	Moderately sorted, coarse- to very coarse-grained, clean sand, gravelly sand and gravel, erosionally based units < 10 m thick, cross-bedding, flat lamination, ripple cross-lamination.
Floodplain	Sand, interbedded sand and mud, with plant debris and roots, older deposits show pedogenic mottling and concretions.
Lower Delta Plain	
Distributary Channel	Poorly sorted, coarse- to very coarse-grained, variably mud-rich sand and gravelly sand, otherwise as for Upper Delta Plain.
Tidal Creek	Poorly sorted, variably mud-rich sands, and muds, erosionally based units 1–3 m thick, ripple cross-lamination and flat lamination, mangrove and other plant debris, shells.
Mangrove Swamp	Root-penetrated, organic-rich, medium to dark gray mud and minor sand, bioturbated, shells.
Salt Flat	Interlaminated mud and fine-grained sand, or pure mud, with salt crystals and crusts, microbial mats.
Other Coastal Flat	Root-penetrated mud, minor sand, mottled gray to brown and pedogenically altered.
Foreshore/Beach Ridge/Spit	Well sorted, medium-grained, clean sand with scattered shell debris, pumice, plant debris, flat lamination and low-angle, seaward-dipping cross-bedding, ripple cross-lamination.
Aeolian Dune	Well sorted, fine- to medium-grained, clean sand, foredunes appear internally structureless, parabolic dunes preserve large-scale cross-bedding (sets < 6 m).
Delta Front	
Mouth Bar	Poorly to moderately sorted, coarse-grained sand with minor gravel, pumice, plant and shell debris, sharp-based units typically 5–8 m thick, internally dominated by flat lamination, low-angle cross-bedding.
Shoal	As above.
Lower Delta Front	Mud, bioturbated with shells and plant debris.
Embayment	Interlaminated and thinly interbedded mud and sand with shells and plant debris.
Prodelta	No modern prodelta recognized. Otherwise, as for Lower Delta Front.
Transgressive Settings	Moderately to well sorted sand and gravel, erosionally based units < 2 m thick, abundant shells.

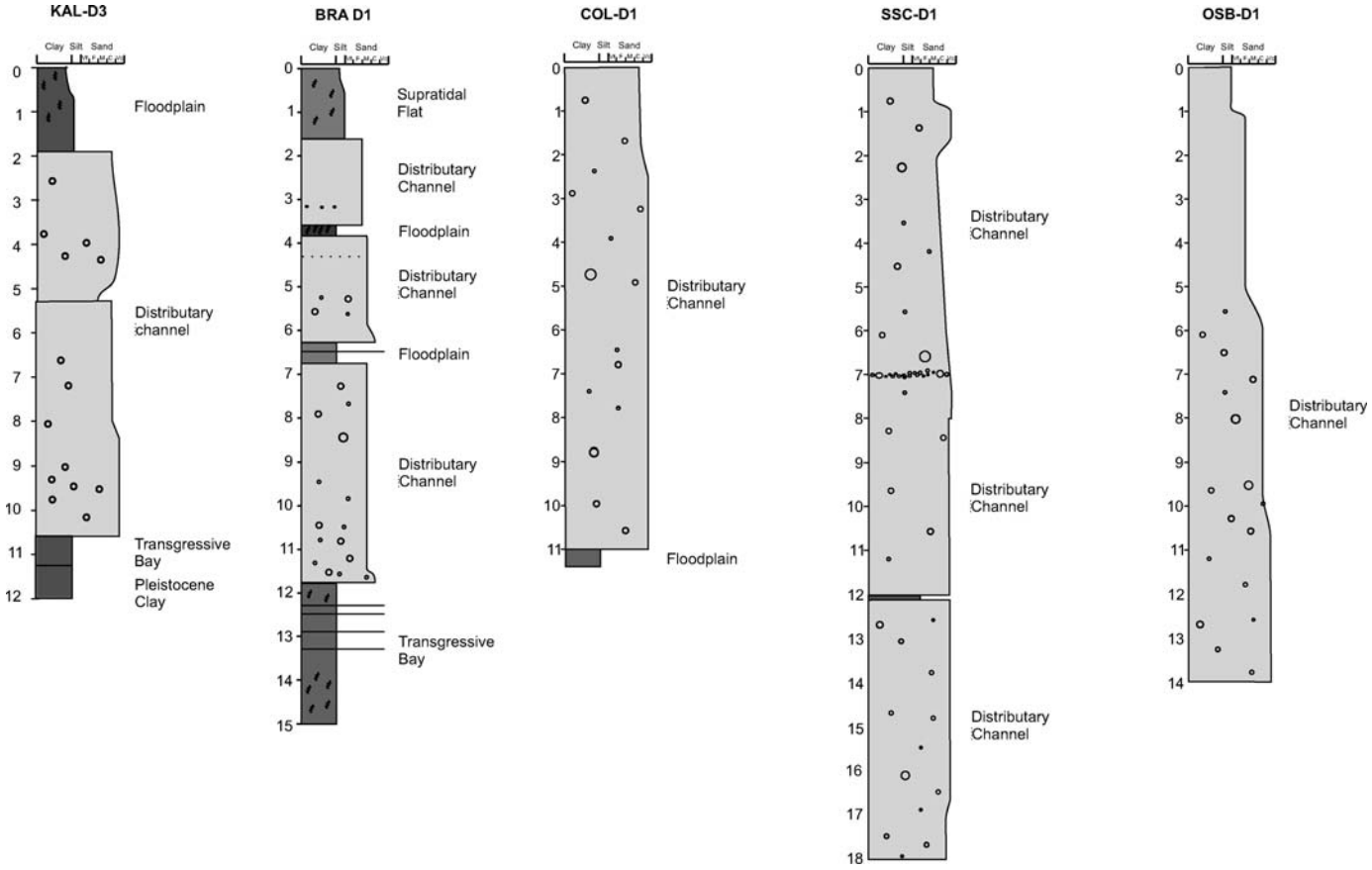

FIG. 3.—Representative graphic logs from holes drilled on the Upper Delta Plain of the Burdekin Delta. The section is dominated by sharp-based bodies of coarse- to very coarse-grained sand and gravelly sand, interpreted as channel deposits. Note the contact between channel sands and underlying interpreted transgressive bay muds near the base of holes KAL-D3 and BRA-D1. See Figure 4 for key to symbols used.

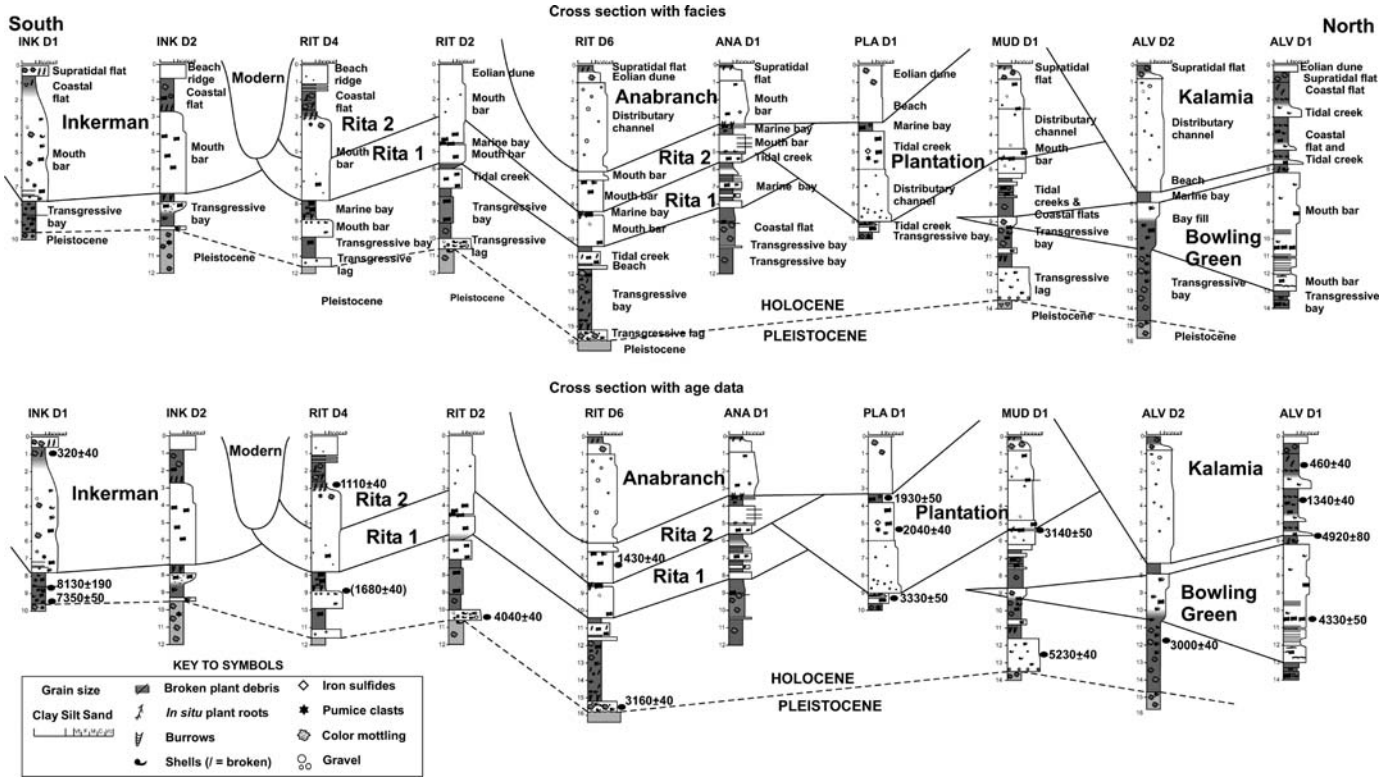

FIG. 4.—Representative graphic logs from holes drilled on the Burdekin Delta Lower Delta Plain. The north–south transect is parallel to the eastern coastline of the delta and thus perpendicular to the trend of distributary channels and associated river-mouth facies. The upper panel shows the facies interpretation of each section, and the definition of discrete sub-deltas based on geomorphic data and radiocarbon ages, and the lower panel emphasizes the radiocarbon ages and correlations.

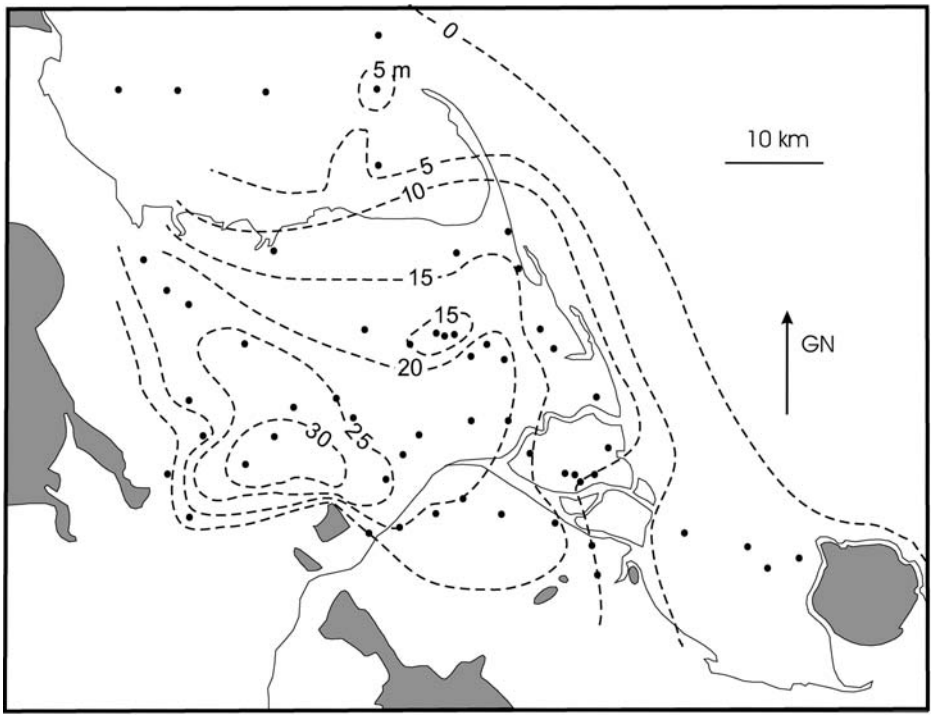

FIG. 5.—Holocene isopach map for the Burdekin River delta (contours in meters), based on drilling undertaken during this study and selected holes from the Irrigation and Water Supply Commission (IWSC) database. Areas shaded gray are exposed bedrock uplands. Note that a significant Pleistocene section underlies the Holocene interval.

TABLE 3.— *Chronology of delta lobes, showing interpreted age ranges.*

Lobe	Name	Age Range (years BP)	Context
13	Modern	< 1000	Slight falling stage and stillstand
12	Anabranch	< 1000	
11	Rita 2	2000–1000	
10	Kalamia	?2000–1000	
9	Gainsford 1 + 2	?2000–1000	
8	Plantation	3000–2000	
7	Jerona	?4000–3000	Highstand
6	Rita 1	4000–3000	
5	Bowling Green	5000–4000	
4	Sheep Station Creek	?7000	Rising sea level
3	Inkerman 1–3	7000–6000	
2	Home Hill	??8000–7000	
1	Barrattas	?10000–8000	

? denotes greater uncertainty and sea-level context.

channels during short-duration high-magnitude runoff events (Fielding et al. 2005a, 2005b), and we describe the delta as "flood-dominated" to reflect this. However, the distribution of radiocarbon ages is such that a simple correlation of sand bodies across the coastal strip is not realistic, and the notion of a simple pattern of progradation is not supported by the data (Fig. 4). From this age distribution, and the preservation of numerous paleochannel courses across the modern delta plain, we submit that the Holocene delta platform has been constructed via the progradation of a number of discrete delta lithosomes. The exact planform geometry of these bodies cannot be determined, and they probably varied through the Holocene according to the degree of exposure to oceanic swell and other wave energy. However, wave action would likely have produced more or less linear shorelines, particularly following abandonment of individual sub-deltas, rather than the more pear-shaped planform typical of river dominated systems. The term "lobe" is used herein as a broad, generic planform descriptor.

The following section establishes the chronology of Holocene delta platform construction via a combination of geomorphological, stratigraphic, and geochronological evidence. Thirteen discrete delta lobes are identified (Table 3), and the sequence of their formation is interpreted in the context of the independently known sea-level history. This builds on Hopley's (1970) work, which predated modern stratigraphic and sedimentological concepts and had relatively few geochronological anchor points from which to determine the age distribution of strata.

ANTECEDENT CONDITIONS—PLEISTOCENE AND EARLIER HISTORY OF THE BURDEKIN RIVER DELTA

Reconstructions of sea level in the west Pacific region through the last glacial cycle (Chappell et al. 1996) suggest a protracted, long-term decline from 125 ka to 18 ka, punctuated by shorter-term and modest rises (Fig. 6A). During the projected sea-level drawdown, the entire Great Barrier Reef shelf would have been exposed, and the lowstand shoreline would have been on the upper continental slope (Woolfe et al. 1998; Dunbar et al. 2000).

Little is known about the early deposits of the area now covered by the Burdekin River delta, although geophysical data and isopachs of the sedimentary section overlying crystalline basement rocks indicate that there is a substantial pre-Holocene sedimentary succession. There seems to be a general presumption that the sedimentary section is entirely Pleistocene (Hopley 1970), and there are no geochronological dates older than 30 ka (Table 1). Basement maps compiled from the drilling database suggest a number of river valleys incised into the mostly granitic bedrock (Fig. 7). Hopley (1970) first recognized these features, and suggested that they were probably cut and filled numerous times over the course of several cycles of sea-level fluctuation. He also drew attention to the exposed bedrock (at about the elevation of modern sea level) in the bed of the Burdekin River at The Rocks (Fig. 1), a narrow constriction between massifs of the Stokes Range to the south and Kelly Mount to the north.

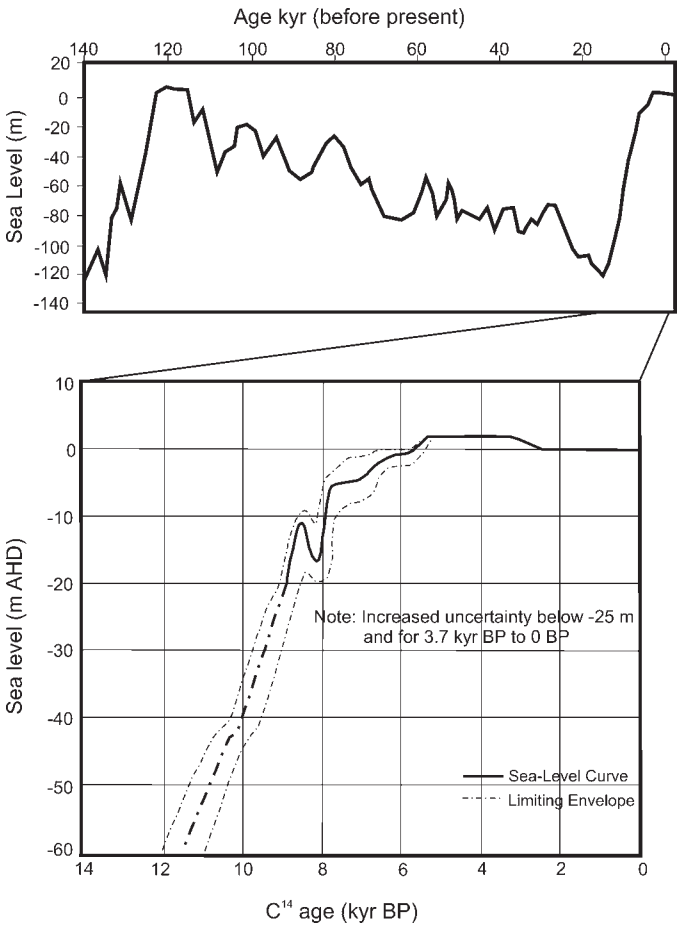

FIG. 6.— Quaternary sea-level history for northeastern Australia. **A)** The last glacial cycle, from Chappell et al. (1996), and **B)** the postglacial sea-level rise, from Larcombe et al. (1995).

It appears that the Burdekin River, until relatively recently, flowed to the north around the west side of Kelly Mount toward or to join the Haughton River. The river could not pass through The Rocks area until the land surface to the west of Kelly Mount was raised relative to The Rocks, and this could have been achieved by (a) Burdekin floodplain aggradation, (b) erosion of The Rocks by a smaller stream draining the eastern side of Kelly Mount and adjacent Stokes range, and/or (c) capture of the upstream Burdekin by the shorter coastal stream.

Pleistocene alluvial and deltaic sediments are preserved in the subsurface of the Burdekin Delta, and there are a number of radiocarbon dates in the range 15–30 ka (Table 1). Furthermore, drillers' logs from IWSC boreholes record "limestone" overlying basement at a number of localities including sites west of The Rocks (Fig. 7), suggesting that the shoreline transgressed a considerable distance inland at times during the Pleistocene or earlier, leaving Kelly Mount and other bedrock massifs as islands or promontories. The IWSC drillers' logs, unfortunately, do not allow clear discrimination between Pleistocene (and older?) strata and Holocene sediments, even given the contrast in consolidation noted above. Thus, mapping of the Pleistocene–Holocene contact is not a simple exercise, and in this study has been achieved by extrapolating from our hollow-stem auger drillholes where the contact was clearly recognizable.

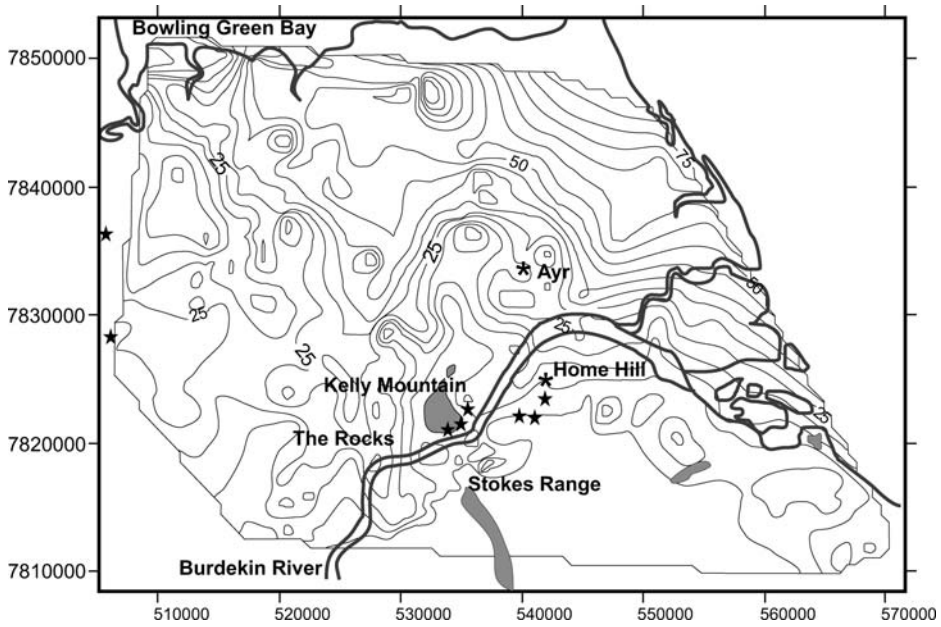

FIG. 7.—Map showing basement elevation in meters below sea level (from Corbett 2000). Contour interval is 5 m. Black stars denote drillers' records of "limestone" (interpreted as carbonate-cemented and shell-rich gravel and sand) in the Pleistocene section, indicative of the extent of Pleistocene marine transgressions. Areas shaded gray are uplands significantly above sea level. Coordinates are for the Australian Map Grid (AMG), Zone 55.

Offshore, stratigraphic patterns are somewhat clearer, although data are mainly confined to seismic reflection records with little or no lithological or geochronological control. Reflector "A" of Orme et al. (1978) and subsequent workers can be traced across the Great Barrier Reef shelf, and is interpreted as a surface exposed by sea-level fall during the last glacial cycle. A number of alluvial channel fills are associated with this surface, and these are believed to record rivers that crossed the shelf towards the falling-stage and lowstand shoreline (Orme et al. 1978; Johnson et al. 1982; Searle 1983; Johnson and Searle 1984; Harris et al. 1990; Carter et al. 1993). From widely spaced seismic reflection data, these authors concluded that the channels crossed the shelf more or less perpendicular to the coast to reach the shelf edge. Woolfe et al. (1998), however, noted that the abundant carbonate reefs on the outer shelf would have been exposed during falling stage and lowstand, and would have presented a topographic barrier to any contemporary rivers. Accordingly, they proposed that rather than crossing the shelf to the lowstand shoreline, rivers might have turned to flow parallel to the coast and discharged into extensive wetlands and lakes formed in the topographic low of the mid-shelf. Fielding et al. (2003, 2005c) traced one prominent paleochannel by seismic reflection surveys from the mouth of the modern Haughton River (Fig. 1) to within 10 km of the shelf edge, demonstrating that at least one lowstand channel did cross virtually the entire shelf. It is likely that this represents one of the major courses of the Burdekin during the last glacial cycle, and it shows cross-sectional form and plan geometry similar to the modern river (Fielding et al. 2003, 2005c).

Available data suggest that the lowstand landscape was an extensive lowland plain, with widely separated rivers cut into a relatively flat well-drained surface. As sea level began to rise following the c. 18 kyr BP lowstand, this lowland plain was progressively (and probably rapidly) flooded.

HOLOCENE DELTA CONSTRUCTION

The Chappell et al. (1996) sea-level model has a simple, postglacial sea-level rise over the last 18 kyr (Fig. 6A). More detailed analysis of postglacial sea level by Larcombe et al. (1995) suggests a somewhat more complex history (Fig. 6B), although this has been disputed by Harris (1999). In the Larcombe et al. (1995) analysis, sea level is interpreted to have risen rapidly until stillstand and short-term drop at 8.5–8 kyr BP. Following this, sea level continued to rise, at first rapidly and then more slowly, until achieving a highstand at about 5.5 kyr BP. The highstand persisted from 5.5 to about 3 kyr BP, following which there was a slight (1–2 m) sea-level drop to the present level, achieved at about 2.5 kyr BP. The oldest Holocene radiocarbon ages from the delta are c. 8 kyr BP, suggesting that delta construction began at or shortly before this time.

Initial Delta Formation During Rising Stage (?10–8 kyr B.P.)

The Holocene succession is no more than c. 25 m thick over the whole extent of the delta plain (Fig. 5). Given this and the Larcombe et al. (1995) sea-level curve, it is likely that the present delta area was flooded by the postglacial transgression at about 10–9 kyr B.P. (Figs. 5, 6B). The extent of the marine transgression can be constrained from drillers' records of shells in the shallow subsurface and from the extent to which transgressive mud identified in our coastal drilling can be extrapolated inland (Fig. 8A). However, given the bedrock constriction at The Rocks (Fig. 1), the course of the Burdekin during the first part of the postglacial sea-level rise must have been northward around the west side of Kelly Mount toward or to join the Haughton River and enter the sea east of the Mount Elliott Range (Fig. 1). This route is likely to have been the principal falling-stage, lowstand, and rising-stage course of the Burdekin River, and it is consistent with the buried paleochannel documented by seismic data offshore (Fielding et al. 2003, 2005c; Fig. 8A).

Hopley (1970) proposed that an early Holocene delta occupied the northwestern part of the delta plain in the area now crossed by the Barratta Creeks (Fig. 1). Although there are no geochronological data to constrain this interpretation, IWSC drilling data indicate a substantial sand-dominated section overlying a basal, presumably marine mud in this area (Corbett 2000). Modern catchment patterns suggest that the early Holocene delta could initially have been supplied predominantly by the Haughton River and that drainage from the Burdekin catchment gradually became more significant, possibly through stream capture. Therefore, it is proposed that during rising sea level the Haughton and Burdekin rivers formed a delta in the northwest corner of the modern delta plain, here named the "Barrattas" delta lobe (Fig. 8A, Table 3). Thus the early Holocene landscape of the modern Burdekin Delta area

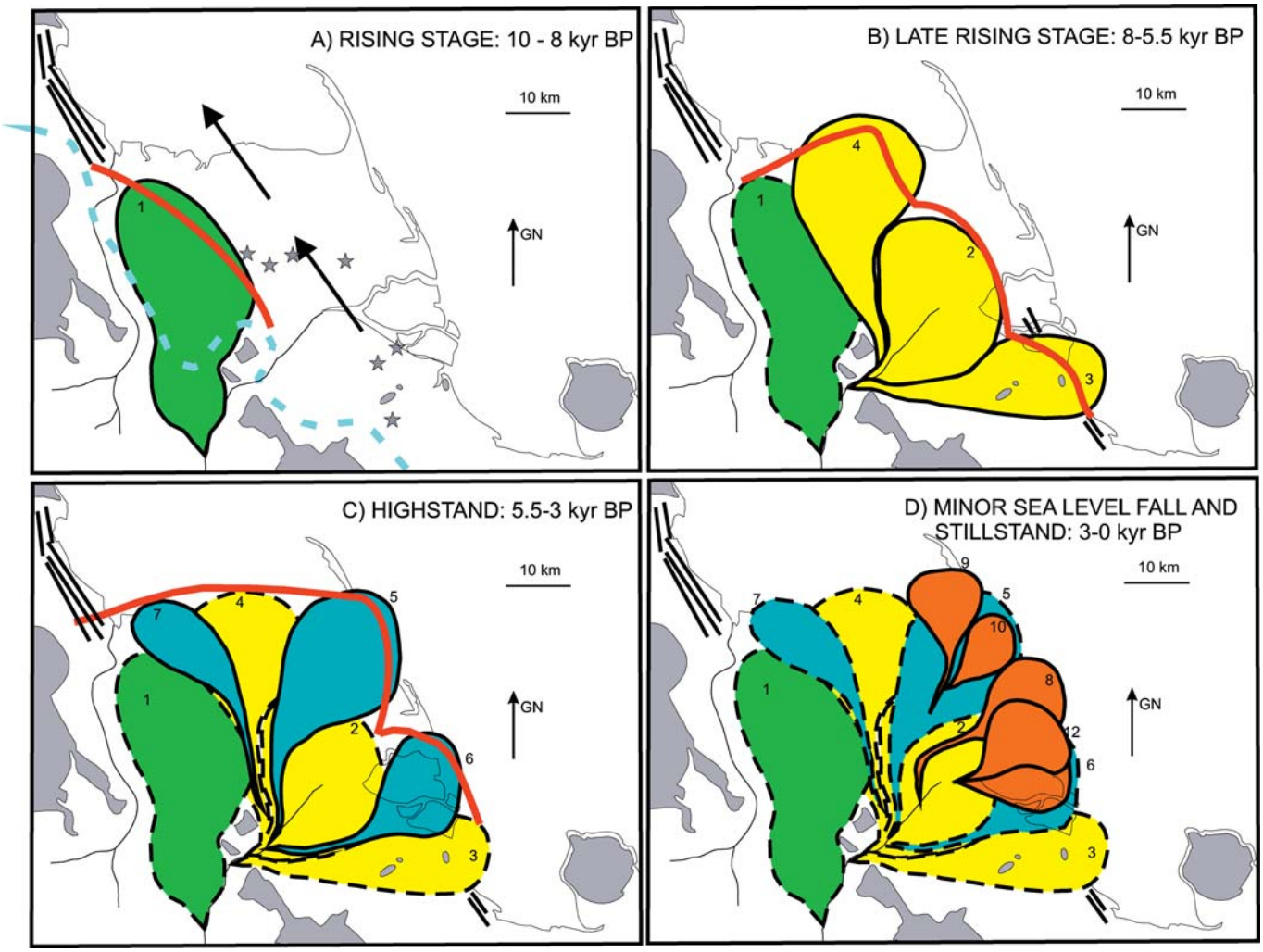

FIG. 8.—Maps showing interpreted paleogeography of the Burdekin River delta **A)** during rising sea level 10–8 kyr B.P., **B)** during slowed rise of sea-level 8–5.5 kyr B.P., **C)** during sea-level highstand 5.5–3 kyr B.P., and **D)** during slight sea-level lowering and stillstand 3–0 kyr B.P. The numbered lobes correspond to those listed and named in Table 3. Stars on the map in Part A denote drillers' records of "seashells" within the basal Holocene section. Thick dashed line on the map in part A indicates interpreted position of the maximum transgression shoreline, at c. 10 kyr B.P. Solid black lines indicate selected flights of linear beach-ridge and foredune complexes (see Fig. 2), indicative of former shoreline positions. Black arrows on the map in Part A emphasize the likely enhanced longshore drift during early Holocene development of the delta, owing to the open nature of the coastline. Solid red lines on the maps in parts A, B and C indicate the likely positions and shapes of shorelines following progradation and abandonment of individual delta lobes, as indicated in part by paleo-beach ridges preserved on the present land surface (Fig. 2). The present coastline was achieved via the reworking of the delta lobes shown on the Map in Part D, including formation of the Cape Bowling Green and other spits. Note the progressive decrease in size of delta lobes through the Holocene.

comprised a backstepping, rising stage delta lobe in the northwest and a large, transgressive marine embayment to the south (Fig. 8A). The early deltaic coastline would have had little protection from the prevailing wave climate, and long-shore currents would have been significant, so that the delta shore would have been largely linear and northwest-oriented (Fig. 8A). This is supported by the presence of extensive sets of linear shoreline ridges of probable early Holocene age along the western shore of Bowling Green Bay (Figs. 2, 8A), which probably were fed by the Barrattas delta lobe.

No stratigraphic record of the c. 5 m sea-level fall at c. 8.5–8 kyr B.P. proposed by Larcombe et al. (1995) can be recognized in the delta, but such a sea-level drop may have acted to help maintain the Burdekin River's course to the west of Kelly Mount by encouraging incision rather than aggradation and avulsion (Fig. 8A). This therefore would be preserved only as elongation of the delta lobe.

Initial Construction of the East-Facing Delta during Late Rising Stage (8–5.5 kyr B.P.)

A number of radiocarbon ages from the subsurface of the delta plain and Upstart Bay (Table 1) indicate that the east-facing delta started to form between 8 and 5.5 kyr B.P. It is likely that an event or events at about 8 kyr B.P., most likely capture of the upstream Burdekin by a smaller stream eroding headward into the east side of The Rocks, contributed to the river avulsing to the east and taking a new course through the bedrock constriction at The Rocks (Fig. 8B). Given that at 8 kyr B.P. sea level was rising rapidly from −15 m to −5 m (Larcombe et al. 1995), the pre-avulsion shoreline would have been directly to the east of the bedrock ridge of Kelly Mount and the Stokes Range (Fig. 8A, B). Avulsion through The Rocks gap at ?8 kyr B.P. would have initiated delta formation immediately east of the gap, with rapid propagation

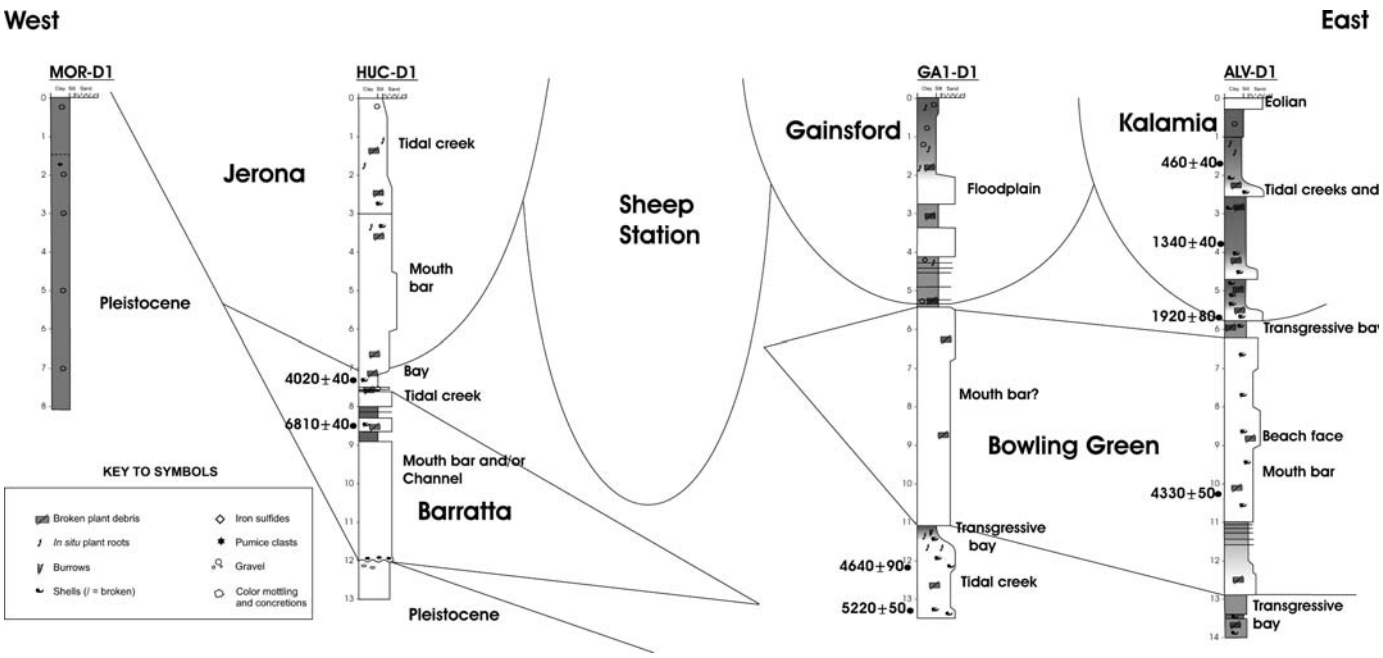

FIG. 9.—West-to-east drilling transect across the north coast of the delta plain (see Fig. 1 for locations of drillholes). Note the complex stratigraphy, similar to that depicted in Figure 4, and the presence of Pleistocene mud at the surface in the far west. Numbers denote radiocarbon ages, expressed as corrected, conventional ages in radiocarbon years BP with one standard deviation error.

eastward into shallow (probably < 5 m) water (Fig. 5). Drilling data confirm a substantial sand-dominated section of probable Holocene age in the subsurface east and northeast of The Rocks, although no radiocarbon dates are available to confirm the exact age of this accumulation. This putative delta lobe (or lobes) is named "Home Hill" after the township built on the resulting delta platform (Fig. 8B, Table 3).

Two other delta lobes (Table 3) are recognized that belong to this initial phase of eastward delta construction, both of which appear to have more elongate planforms than the Home Hill lobe, and to have occupied the accommodation space either side of that lobe as sea level rose to -5 m. The presumed earlier of these lobes (constrained by radiocarbon ages of 7350 $\pm$ 50 yr B.P. and 8130 $\pm$ 190 yr B.P. from the base of drillhole INK-D1; Fig. 4, Table 1) was constructed to the south and southeast of the Home Hill lobe by the river avulsing to a series of courses running around the northern boundary of the Stokes Range uplands. The remnants of these courses are visible on the surface (Figs. 1, 8B) and indicate the extent and position of the "Inkerman" lobe. A radiocarbon age of 6560 $\pm$ 40 yr B.P. from a shell recovered in subsurface mud in Upstart Bay confirms that delta-front and prodelta deposits were accumulating in Upstart Bay at this time. Remnants of ancient beach-ridge systems have been mapped along both the northern and southern flanks of the Inkerman delta lobe (Figs. 2, 8B), and suggest the refraction of waves driven by the southeasterly winds around the bedrock massif of Cape Upstart, which at this time was probably still an island (Fig. 8B). The Inkerman delta lobe was protected from the prevailing winds and waves by Cape Upstart, and this partly explains its elongate planform and, together with subsequently low sedimentation rates, accounts for the pristine preservation of its landforms on the modern surface.

A slightly younger delta lobe is recognized to the north and northwest of the Home Hill lobe. The "Sheep Station Creek" delta lobe is constrained by a radiocarbon age of 6810 $\pm$ 40 yr B.P. from a mud unit above a thick, mouth-bar and/or channel sand body in drillhole HUC-D1 (Figs. 1, 8B, 9). Remnants of the channels interpreted at the distributaries of this delta lobe are preserved on the surface as Sheep Station Creek (after which the delta lobe is named), and tributaries and small remnants of beach ridge systems mapped near the modern northern coast may have formed during this time (Figs. 1, 8B). It seems likely that the Sheep Station Creek delta lobe exploited a depression between the older Barrattas and Home Hill lobes and prograded farther northward into shallow water. Sand from this lobe would have nourished the beach ridges along the northwest coast via vigorous longshore drift because the lobe front was not protected by Cape Upstart from the prevailing wind (Fig. 8B). The delta-front clinoforms of the Sheep Station Creek lobe are preserved under eastern Bowling Green Bay, demonstrating progradation into c. 13 m of water.

A lack of radiocarbon ages from 6500–5500 yr B.P. in our database (Table 1) suggests that no new lobes formed in this interval, and that the Inkerman and/or Sheep Station Creek lobes remained active through the final slowing of sea-level rise to the highstand at 5500 yr B.P. (Fig. 6). By this time, the basic planform of the modern delta had formed (minus Cape Bowling Green; see below) and was probably strongly asymmetric due to the vigorous northwestward longshore drift (Fig. 8B). The succeeding highstand delta lobes had to overstep these rising stage lobes to discharge their water and sediment loads at the coast.

Enlargement of the Delta Platform during Highstand (5.5–3 kyr B.P.)

Three delta lobes are recognized in the subsurface and at the surface, recording the period 5500–3000 yr B.P., the interpreted span of the +1 to +1.5 m highstand (Larcombe et al. 1995). These are somewhat smaller (both in area and in volume) than their rising-stage predecessors, and remnants of their channel systems are preserved on the modern upper-delta-plain surface because the channels crossed the preexisting delta platform with negligible aggradation and there has been minimal aggradation of the areas since (Table 3, Figs. 1, 8C). Some of these channel traces show evidence of dichotomous branching near the coast, indicating that they became distributaries downstream (Fig. 1). The sediments of these three lobes have been extensively intersected by drilling (Fig. 4) and imaged in offshore seismic reflection profiles, indicating that

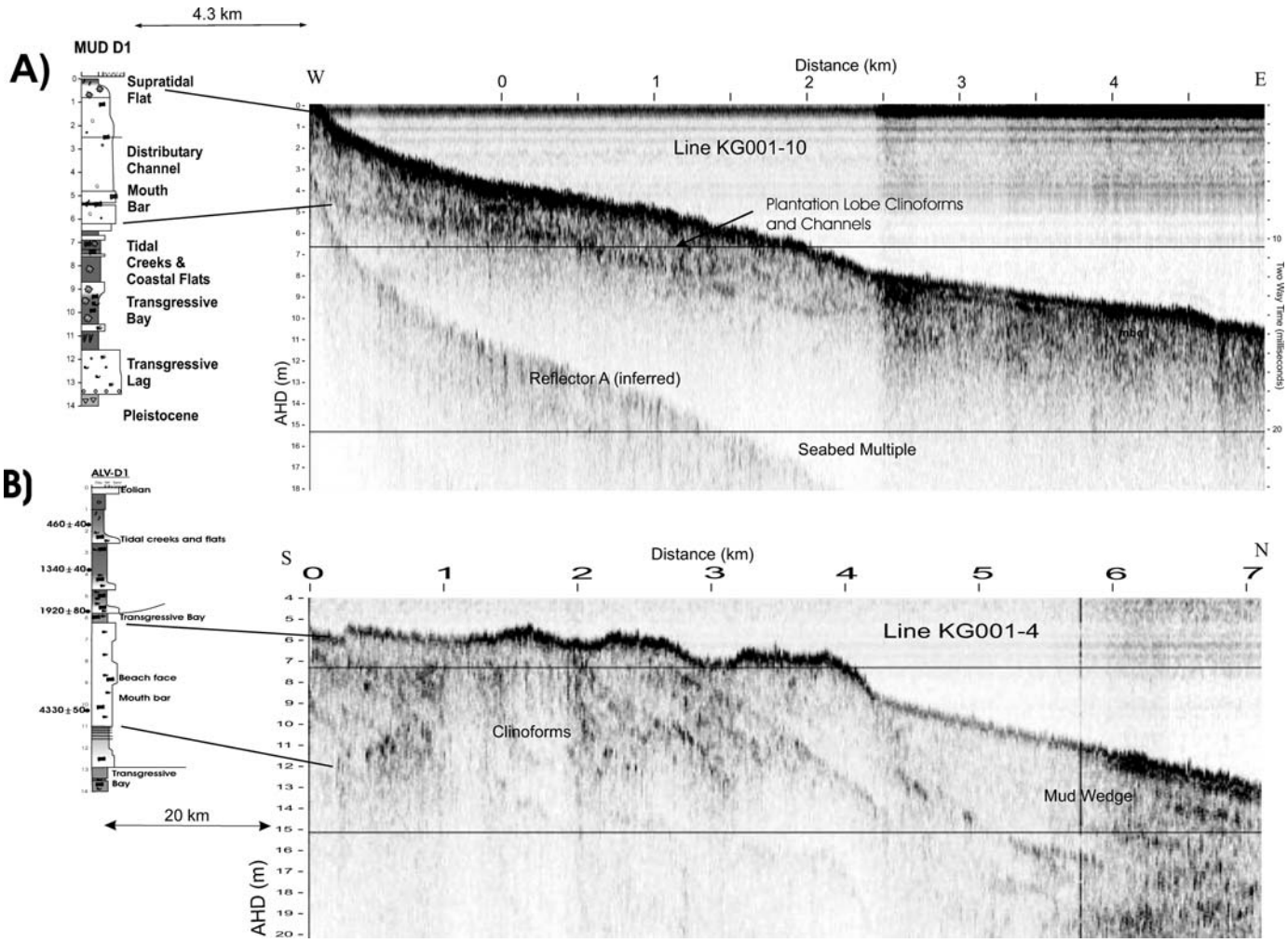

FIG. 10.—Seismic images across **A)** the Plantation delta system and **B)** the Bowling Green delta system (Table 3), showing in each case the prominence of clinoform seismic facies representative of paleo-delta fronts.

the original eastward extent of the highstand delta was somewhat greater than the modern-day delta.

The first highstand delta lobe was the largest, and formed on the northeast coast between the older Sheep Station Creek and Home Hill lobes (Fig. 8C). This "Bowling Green" lobe is constrained by radiocarbon ages from strata underlying and overlying the sand body, and by an age of 4330 ± 50 yr B.P. from within the sand body in drillhole ALV-D1 (Figs. 1, 4, 9). It is likely that this lobe was fed by a channel that was later partly reoccupied by Kalamia Creek, and remnants of it are extensively preserved, for example under the township of Ayr (Fig. 1). Much of the Bowling Green lobe is preserved in the subsurface, both onshore (Figs. 4, 9) and offshore (Fig. 10B). The gradationally or sharply based sand bodies encountered in drilling (Figs. 4, 9) are interpreted as channel and mouth-bar deposits, while the clinoforms evident in seismic line KG001-4 (Fig. 10B) are interpreted as sandy mouth-bar facies passing distally into muddy lower-delta-front facies (cf. Fielding et al. 2005b).

The second highstand lobe is located somewhat to the south of the Bowling Green lobe, and evidently reached the coast through a depression between the older Home Hill and Inkerman lobes (Fig. 8C). The "Rita 1" lobe was recognized in drillhole logs and geophysical data from the eastern end of Rita Island (Figs. 1, 4, 11, figure 7 of Fielding et al. 2005b). Clinoforms evident in seismic line KG00-01-11 (Trueman 2002) probably record remnants of this lobe. Radiocarbon ages constrain the Rita 1 lobe to 4–3 kyr B.P. (Fig. 11). Geomorphic patterns on the modern delta-plain surface suggest that the Rita 1 lobe may have been fed by a channel that at least partially reoccupied one of the earlier Inkerman channel courses, turning northeast as it approached the coast to exploit a depression between two older lobes (Figs. 1, 8C).

The third highstand lobe (Fig. 8C), located in the far northwest of the Holocene delta plain, partially overlies and oversteps the earlier Sheep Station Creek lobe. The "Jerona" lobe is somewhat narrower and smaller in area than its predecessors (Fig. 8C) and may have been fed by reoccupation of the Sheep Station Creek and Collinson's channels, which preserve evidence of multiple avulsion points and of lateral channel migration (Fig. 2). In addition to surface observations, evidence for the Jerona lobe comes from drillhole logs (Fig. 9), where a 7-m-thick, composite sand body overlies shell-rich muds that yielded a radiocarbon age of 4020 ± 40 yr B.P. The Jerona lobe is thus younger than 4 ka, and is the youngest substantial deltaic depocenter to have formed on the northwest coast before the most recent phase of delta construction on the east coast (Fig. 8D). We suggest that the Jerona lobe records a period similar to that of the Rita 1 system, 4–3 kyr B.P. (Table 3). Although there is little definitive evidence as to which of the two lobes (Rita 1 and Jerona) formed earlier, it is unlikely that they formed at the same time.

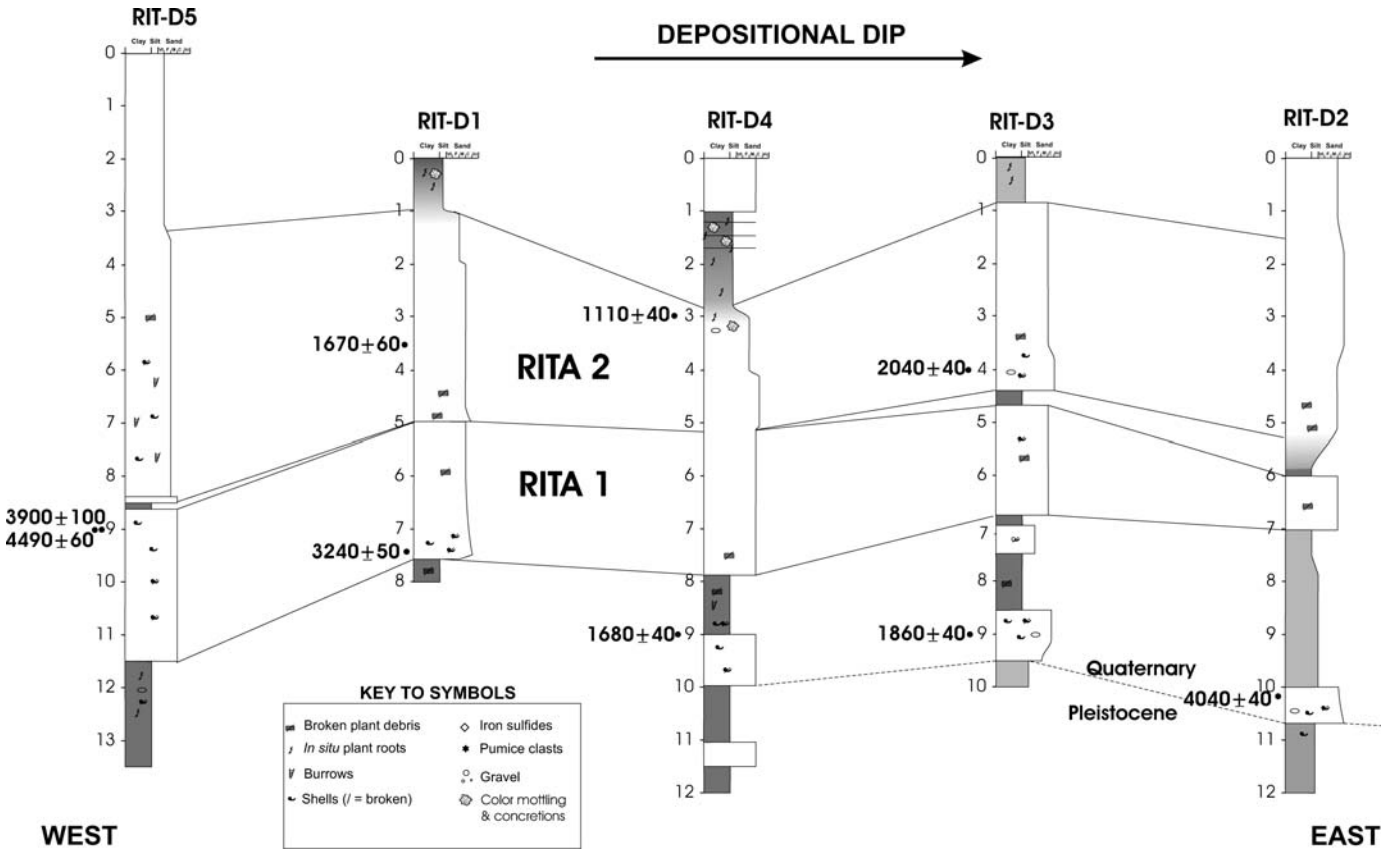

FIG. 11.—West-to-east drilling transect across the southern edge of Rita Island, on the Lower Delta Plain (see Fig. 1 for locations of drillholes). Numbers denote radiocarbon ages, expressed as corrected, conventional ages in radiocarbon years BP with one standard deviation error. Note the penetration of the Pleistocene–Holocene interface in the more easterly holes, the basal coarse-grained lag above the unconformity, and the lateral continuity of the Rita 1 and Rita 2 delta deposits in the depositional dip direction. The older Rita 1 lobe thins significantly towards the seaward (eastern) end of the transect. Note also some internal inconsistency among radiocarbon ages, suggesting reworking of organic debris.

Thus by the end of the highstand at c. 3 kyr B.P., the present form of the Burdekin Delta plain was more or less established.

Smaller Delta Lobes Formed during Stillstand and Minor Sea-Level Fall (< 3 kyr B.P.)

A suite of six smaller delta lobes records the last 3 kyr of delta construction (Table 3, Fig. 8D). All of these lobes are located on the eastern and northeastern coast of the delta, and were fed by channels that crossed older delta deposits without significant delta-plain aggradation (Fig. 8D), such that these young channel courses are the most readily recognizable on the modern delta plain, clearly visible on the ground and from the air. Many radiocarbon ages (Table 1), drillhole data (Figs. 3, 9, 11), and surface mapping data (Figs. 1, 2) constrain these delta lobes, although some of their ages must be inferred from crosscutting relationships evident on the modern surface. Remnants of broadly northwest-elongate beach-ridge and eolian dune systems are preserved on the present delta plain that record northwestward longshore sediment transport from these paleo–river mouths (Fig. 2).

The oldest of the lower stillstand lobes is recognized in the central part of the eastern coast, and is believed to have been fed by a channel that is now followed by Plantation Creek (Figs. 1, 8D). The "Plantation" lobe is constrained by radiocarbon ages to 3–2 kyr B.P. (Fig. 4), and clinoform reflectors on seismic line KG00-01-10 represent the lobe front 4–5 km outboard from the modern beach, passing distally (5–8 km) into flatter and planar reflectors of the prodelta (Fig. 10A). The maximum extent of progradation of the Plantation lobe was considerably seaward of the present coastline, implying coastline retreat following lobe abandonment.

The second lobe in this group formed farther to the north, issuing into what is now the northeast corner of Bowling Green Bay and Cape Bowling Green (Fig. 8D). Radiocarbon ages constrain this "Gainsford" lobe to about 2–1 kyr B.P. (Fig. 9), and geomorphological patterns suggest that the Gainsford channel is now partly occupied by Kalamia Creek but turns northward west of the township of Alva (Fig. 1). Sand delivered to this lobe, and perhaps also to its successor the Kalamia lobe, formed Cape Bowling Green, which from radiocarbon ages appears to be c. 1 kyr old (Table 1). Northwest-trending beach-ridge and dune complexes now stranded on the lower delta plain west of Alva (Figs. 1, 2) indicate positions and trends of the shoreline prior to growth of Cape Bowling Green. The succeeding Kalamia lobe formed following avulsion of the Gainsford channel at a point near Alva to form the coastal portion of paleochannel now followed by Kalamia Creek (Fig. 1). The Kalamia lobe is constrained by radiocarbon ages and crosscutting relationships to a timeframe similar to that of the preceding Gainsford system, i.e., 2–1 kyr B.P. (Figs. 1, 4) and would have started to form before the Gainsford lobe was entirely abandoned (by comparison with recent history of the modern Burdekin River mouth).

The next small delta lobe formed farther south, and gave rise to much of the land surface now making up Rita Island. The "Rita 2" lobe (Fig. 8D) partially buried the Rita 1 lobe, presumably occupying

accommodation space formed by the abandonment, consolidation, and subsidence of the earlier lobe. The stacking of channel and mouth-bar sand bodies can be seen clearly in borehole logs and in ground-penetrating radar data (Fig. 11; figure 7 of Fielding et al. 2005b). The Rita 2 lobe was also active 2–1 kyr B.P., and was fed by a precursor of the modern Burdekin River channel. Geomorphic features attributable to this lobe are still well preserved on the modern lower delta plain, notably remnants of well-preserved sets of beach ridges with associated parabolic eolian dunes (Fig. 2). These ridges are truncated to the north by deposits of the succeeding lobe, named "Anabranch" after its (still partially extant) channel (Fig. 8D). The Anabranch lobe is $<$ 1 ka in age, from radiocarbon ages and crosscutting relationships, and is being succeeded by the modern, active delta lobe which has truncated the Rita 2 lobe beach ridges to the south (Figs. 2, 8D). A series of spits along the eastern coast of the modern delta (including Cape Bowling Green) are interpreted to have formed perhaps coevally over the most recent 1–2 kyr, in response to gradual abandonment and retreat of the small, east coast delta lobes, and reworking of sands by longshore drift (Fig. 2). Most recently, two such spits have formed and are migrating rapidly along the coast (Pringle 2000). Evidence of coastal retreat along the east coast is extensively preserved as exposed mangrove flat muds that are being exhumed on present-day beaches (e.g., northward from Alva, and south of the modern river mouth).

SUMMARY OF HOLOCENE DELTA HISTORY AND STRATIGRAPHY

From the foregoing, it is clear that the Holocene Burdekin River delta has been constructed via a series of discrete bodies, beginning at perhaps c. 10 kyr B.P. when sea level had risen from c. −120 m to c. −40 m (Fig. 6). The patterns of sediment dispersal in time and space evidently were not random, and were somewhat predictable given antecedent topography and the independently known sea-level history (Larcombe et al. 1995). Prior to c. 8 kyr B.P., fluvial sediments were dispersed to the northwest part of the delta, via a route that turned north inland of The Rocks. Sea level rose rapidly, forming a large, open coastal embayment over much of what is now the coastal plain. Following breaching of the bedrock constriction perhaps c. 8 kyr B.P., construction of the eastern delta began with a series of large lobes fed by a channel that avulsed repeatedly at a node immediately east of The Rocks (Fig. 1). The largest lobes formed from 10 to 5.5 kyr B.P., when sea level was still rising, and these were succeeded by somewhat smaller lobes during the highstand (5.5–3 kyr B.P.). A series of still smaller lobes formed over the last 3 kyr, during a suspected 1–1.5 m sea-level fall and stillstand (Fig. 6). These falling stage to stillstand lobes are all on the eastern coast of the delta and culminate in the modern lobe, which faces eastward into Upstart Bay (Fig. 1).

The thirteen delta lobes formed over c. 10 kyr giving an average avulsion period of c. 750 yr. The depositional patterns (earliest lobes the largest and lobe size declining through time), however, suggest that sediment flux was not constant throughout this interval, and/or that avulsion periodicity changed and sediment dispersion patterns differed. The lobes formed after c. 4 kyr B.P., and especially those formed after 3.5 kyr B.P., are conspicuously smaller than earlier delta lobes. Furthermore, the (admittedly imprecise) age ranges of individual lobes suggest that the inter-avulsion period has decreased through time. The progressive decrease in inter-avulsion period could be related to the slowing rate of change of sea level, in that reduced rate of creation of accommodation space could have led to more frequent avulsion and thus smaller lobe volume. However, because some recent work suggests a positive relationship between avulsion frequency and base-level rise (e.g., Tőrnqvist 1994; Stouthamer and Berendsen 2001), it seems more likely that other factors were influential. For example, changed discharge patterns with fewer but more erratic and larger individual runoff events in the post-4-kyr B.P. strengthened ENSO (El Niño-Southern Oscillation) regime could have facilitated more frequent avulsion. Additionally, as the entire delta edifice extended farther seaward, more frequent avulsion might be expected as (a) the mean gradient decreased, and (b) the length of channels increased, thereby creating more sites for avulsion.

Borehole data indicate that each Holocene delta lobe gave rise to a generally sharp-based, composite sand body dominated by mouth-bar and channel deposits, typically 5–8 m thick, that abruptly overlies the mud deposited during the postglacial transgression, or locally, older subsiding delta-lobe deposits. The Holocene succession of the Burdekin River delta thus comprises a locally developed, coarse-grained basal transgressive lag, overlain by a transgressive mud, in turn overlain by a sand-dominated delta front and delta top deposit (Fig. 12). The age of the top of the transgressive mud varies considerably over the area, depending on the timing of lobe formation.

Assuming that the present sea-level high is a true interglacial (and not a short-lived inflection on a longer-term trend), then the Holocene section constitutes much of a *sequence* in the genetic sense, in which the Pleistocene–Holocene interface with local channel incision ("Reflector A" of Orme et al. 1978) represents the sequence boundary, the basal lag and overlying muds record the transgressive systems tract, and the sand-dominated delta deposits record the highstand systems tract (Fig. 12). Note that the transgressive mud, which extends a considerable distance inland, would be picked as a maximum flooding surface in a sequence stratigraphic analysis, yet its age does not correspond to the time of the highstand, as is predicted by sequence stratigraphic models (e.g., Van Wagoner et al. 1990). In an analysis of an equivalent ancient succession, this distinction would be difficult to recognize, however, because the difference in age between the onset of deltaic sand deposition and the onset of highstand is only c. 5 kyr. Furthermore, the total thickness of the Holocene sequence is only 10–25 m over much of the delta plain, considerably thinner than the typical perception of a sequence (e.g., Emery and Myers 1996; Coe 2003). Indeed, the thickness of the Holocene Burdekin Delta succession is at the vertical scale typically referred to as a "parasequence" (cf. Van Wagoner et al. 1990), despite it having formed following a eustatic sea-level cycle with an amplitude of c. 130 m (Chappell et al. 1996).

DISCUSSION

The Holocene history of the Burdekin River delta summarized above could be interpreted purely in terms of the progressive filling of available accommodation space during the postglacial sea-level rise and highstand. A variety of evidence, however, suggests that the climate of northeastern Australia has varied through the Holocene, and changes in rainfall patterns would have had considerable impact on sediment flux and thus delta growth.

Pollen records (Kershaw 1978; Shulmeister 1992), paleo-plunge-pool deposits (Nott and Price 1994), and alluvial (Wyrwoll and Miller 2001) and arid-zone lake (Magee et al. 2004) stratigraphies all indicate that the tropical north of Australia was wetter during the early Holocene (c. 12–4 kyr B.P.) and became drier subsequently. Several studies both from within Australia (e.g., Nott and Price 1994; Wyrwoll and Miller 2001; Magee et al. 2004; Miller et al. 2005) and from the Asia–Pacific region (e.g., Clement et al. 2000; Goodbred and Kuehl 2000; Bookhagen et al. 2005) have related the early Holocene pluvial period to a strengthened summer monsoon and suppression of the El Niño-Southern Oscillation (ENSO). The reestablishment of strong ENSO is believed to have occurred 4–5 kyr B.P. (e.g., Nanson et al. 1991; Clement et al. 2000; Gomez et al. 2004), and there is little agreement on whether or not these patterns are ultimately controlled by orbital forcing (see discussion in Hesse et al. 2004).

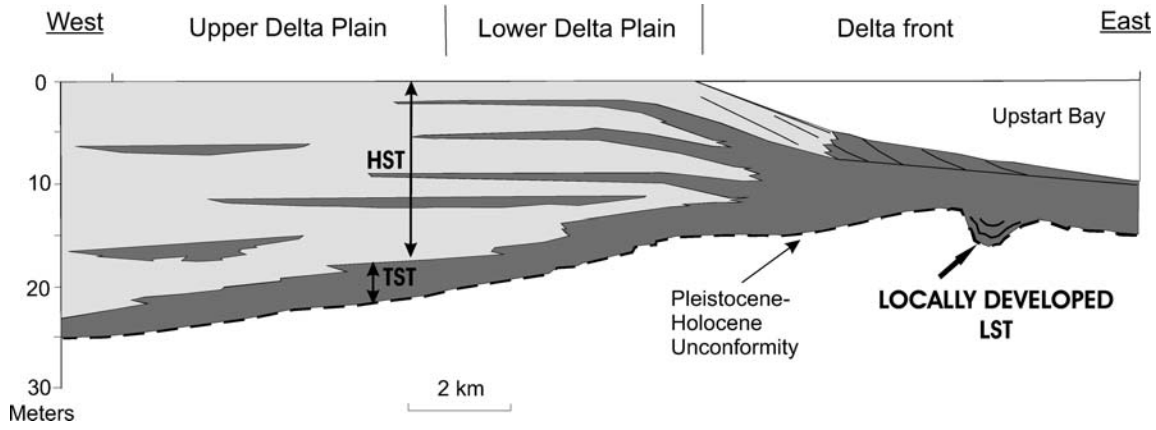

FIG. 12.—Idealized cross section in a dip direction across the Burdekin Delta, showing the Holocene succession as a thin, sand-dominated sequence bounded at its base by the Pleistocene–Holocene interface, a sequence boundary. Note the distribution of systems tracts, with the lowstand systems tract (LST) only locally developed, the transgressive systems tract (TST) recorded by the basal mud unit, and the highstand systems tract (HST) recorded by the upper sand lobes. (light gray = sand, dark gray = mud).

It is tempting to relate the onset of development of the Holocene Burdekin Delta to the early Holocene pluvial phase. Pollen records from Lynch's Crater in the Atherton Tablelands (close to the northern headwaters of the Burdekin River; Fig. 1) indicate an increase in precipitation from c. 11 to c. 7 kyr B.P. (Kershaw 1978; 1983), and our records of the Burdekin Delta suggest that significant sediment accumulation began c. 10 kyr B.P. Increased precipitation would have led to increased runoff, and although this change could also have led to increased vegetation cover and thus decreased erosion rates, other studies (cited above) from the region suggest that sediment yield increased and the climate change led to greater sediment flux down the alluvial valley onto the coastal plain. The end of the wet phase and close of ENSO suppression, estimated at 4–5 ka, coincides closely with the change from large to much smaller delta lobes, and it is conceivable that the return to drier conditions caused the noted change in sediment dispersal. If these relationships are confirmed, then it is likely that significant volumes of coarse sediment were sequestered on the delta plain during the early Holocene, c. 10–5 kyr B.P., in a manner similar to that described for the Ganges–Brahmaputra delta by Goodbred and Kuehl (2000).

It is also probable that stream capture played an important role in initiating the Holocene Burdekin Delta. Firstly, flow must have been diverted from the Haughton drainage system into the Burdekin system, some time during the early Holocene. Secondly, it is probable that breaching of The Rocks may have been facilitated by the headward erosion of a short, steep stream into the eastern side of the bedrock ridge, and capture of the Burdekin flow at The Rocks. Indeed, the bedrock constriction at The Rocks likely played a crucial role in the construction of the Holocene delta, as it negated the formation of an elongate, incised valley in the lower reaches of the river during lowstand. This in turn may explain why the Holocene Burdekin River delta was constructed as a series of discrete lobes rather than as a single progradational front, as has been suggested for some large deltas in Southeast Asia (e.g., Ta et al. 2002; Hori et al. 2002).

CONCLUSIONS

The Burdekin River has constructed a substantial delta during the Holocene. The vertical succession deposited by this delta is typically 10–20 m thick, and comprises (1) a basal, coarse-grained, transgressive lag overlying a continental omission surface (sequence boundary), overlain by (2) a mud interval deposited as the present coastal region was inundated by the rising sea, in turn overlain by (3) a generally sharp-based sand unit deposited principally in channel and mouth-bar settings with lesser volumes of floodplain and beach sediment. Although the planform of the delta is broadly arcuate, suggestive of a strong wave influence, the dominant processes responsible for construction of the Holocene delta are related to major runoff events, and waves only modify the shoreline (after each pulse of flood-generated progradation). The Holocene succession constitutes a sequence in the genetic sense, bounded by the last glacial erosion surface at the base (Reflector A), with only local preservation of potential lowstand systems tract where channels have been entrenched into this surface. There is a more substantial transgressive systems tract consisting of the basal lag and overlying mud, and a highstand systems tract consisting of the upper sand-dominated section. The vertical scale and facies stacking patterns of this succession are suggestive of sediment accumulation at the parasequence scale, although this interval records a true sequence forced by a eustatic cycle of sea-level fall and rise with c. 130 m amplitude.

The Holocene Burdekin River delta was constructed as a series of discrete lobes, formed as the river avulsed. At least thirteen such lobes are recognized, recording the period 10 kyr B.P. to present. Each delta lobe consists of a composite sand body that is typically 5–8 m thick. The earlier lobes that were formed during rising sea level (10–5.5 kyr B.P.) are larger than those formed during the sea-level highstand (5.5–3 kyr B.P.), and significantly larger than those during the past 3 kyr as sea level dropped slightly to its present stillstand. Radiocarbon ages suggest that as the average size of delta lobes has decreased through time the average inter-avulsion period has also decreased. An overlying climatic control of sediment flux is suggested from known paleoclimatic records, and a wetter period 12–4 kyr B.P. coincides with the significantly larger early to mid-Holocene lobes, and the subsequent drier period with the smaller, younger lobes. Increased rates of avulsion in the past 3 kyr coincide with a slowing rate of creation of accommodation. Avulsion period depends in a complex way on several factors and is not necessarily directly related to accommodation (e.g., Bridge 2003). In this case, the shorter avulsion period may be related to one or more of (a) changed discharge patterns with perhaps fewer but larger individual runoff events more often out of equilibrium with the channel form, (b) greater channel length because of progradation of the delta seaward, allowing more sites for avulsion, and (c) an associated decrease in stream gradient.

This paper highlights some of the stratigraphic complexities of deltas formed in shallow water under conditions of limited accommodation. The

vertical sequences and stacking patterns of the Burdekin Delta are dissimilar to those widely regarded as typical of deltaic successions, and they show an internal complexity that is generally under-appreciated. It is hoped that this will stimulate further work on the stratigraphy of shallow-water deltas, towards more detailed facies models for this under-documented class of depositional system.

ACKNOWLEDGMENTS

This research was funded initially by a grant to JA and CRF by BP Exploration Company Ltd. Subsequent research grants from the Australian Research Council (A39937196) to CRF and the Natural Environmental Research Council (GR9/4758) to JA are also gratefully acknowledged. It is our pleasure to record the collaboration and assistance offered us by the Queensland Department of Natural Resources and Mines hydrographers (particularly Geoff Pocock and Tony Horn), the Australian Institute of Marine Sciences (Gregg Brunskill), the James Cook University of North Queensland (driller Paul Givney, technology specialist Kevin Hooper, and ship's master Don Battersby), Terradat Geophysics (Jonothan Thomas), Sunwater, and many other organizations and individuals. We thank Peter Crosdale and the late Ken Woolfe for advice on aquatic creatures and assistance with small boats, and numerous landowners for allowing access to their properties. Kathryn Amos, Ben Corbett, Renee Harvey, Katsuhiro Nakayama, and Matt Petersen participated in field work. Cody Jacobs and Jon Allen at University of Nebraska–Lincoln assisted in the preparation of diagrams. JSR referees Colin Woodroffe and Irina Overeem, Associate Editor Joe Lambiase, and Co-Editor Colin North are thanked for their constructive reviews of the submitted manuscript, and John Southard is thanked for his meticulous copy-editing.

REFERENCES

Alexander, J., and Fielding, C.R., 2006, Coarse-grained floodplain deposits in the seasonal tropics: towards a better facies model: Journal of Sedimentary Research, v. 76, p.

Alexander, J., Fielding, C.R., and Pocock, G.D., 1999, Flood behaviour of the Burdekin River, tropical north Queensland, Australia, *in* Alexander, J., and Marriott, S.B., eds., Floodplains: Interdisciplinary Approaches: Geological Society of London, Special Publication 163, p. 27–40.

Amos, K.J., Alexander, J., Horn, A., Pocock, G.D., and Fielding, C.R., 2004, Supply-limited sediment transport in a high discharge event of the tropical Burdekin River, north Queensland, Australia: Sedimentology, v. 51, p. 145–162.

Belperio, A.P., 1978. An inner shelf sedimentation model for the Townsville region, Great Barrier Reef Province [unpublished Ph.D. Thesis]: James Cook University: Townsville, 230 p.

Belperio, A.P., 1983, Terrigenous sedimentation in the central Great Barrier Reef Lagoon: a model from the Burdekin region: Australia, Bureau of Mineral Resources, Journal of Australian Geology and Geophysics, v. 8, p. 179–190.

Bookhagen, B., Thiede, R.C., and Strecker, M.R., 2005, Late Quaternary intensified monsoon phases control landscape evolution in the northwest Himalaya: Geology, v. 33, p. 149–152.

Bridge, J.S., 2003, Rivers and Floodplains, Forms, Processes, and Sedimentary Record; Oxford, U.K., Blackwell Science, 491 p.

Carter, R.M., Johnson, D.P., and Hooper, K.G., 1993, Episodic post-glacial sea-level rise and the sedimentary evolution of a tropical continental embayment (Cleveland Bay, Great Barrier Reef shelf, Australia): Australian Journal of Earth Sciences, v. 40, p. 229–255.

Chappell, J., Omura, A., Ezat, T., McCulloch, M., Pandolfi, J., Ota, Y., and Pillans, B., 1996, Reconciliation of late Quaternary sea levels derived from coral terraces at Huon Peninsula with deep sea oxygen isotope records: Earth and Planetary Science Letters, v. 141, p. 227–236.

Clement, A.C., Seager, R., and Cane, M.A., 2000, Suppression of El Niño during the mid-Holocene by changes in Earth's orbit: Paleoceanography, v. 15, p. 731–737.

Coe, A.L., ed., 2003, The Sedimentary Record of Sea-Level Change: Cambridge, U.K., Open University/Cambridge University Press, 288 p.

Coleman, J.M., and Wright, L.D., 1975, Modern river deltas: variability of processes and sand bodies, *in* Broussard, M.L., ed., Deltas: Models for Exploration: Houston, Houston Geological Society, p. 99–149.

Corbett, B.J., 2000. Quaternary evolution of the Burdekin Delta, northeast Queensland [unpublished Honours Thesis]: University of Queensland, Brisbane, 85 p.

Donaldson, A.C., Martin, R.H., and Kanes, W.H., 1970, Holocene Guadalupe Delta of Texas Gulf Coast, *in* Morgan, J.P., ed., Deltaic Sedimentation: SEPM, Special Publication 15, p. 107–137.

Dunbar, G.B., Dickens, G.R., and Carter, R.M., 2000, Sediment flux across the Great Barrier Reef shelf to the Queensland Trough over the last 300 ky: Sedimentary Geology, v. 133, p. 49–92.

Emery, D., and Myers, K.J., 1996. Sequence Stratigraphy: Oxford, U.K., Blackwell Science, 297 p.

Farrell, K.M., 2001, Geomorphology, facies architecture, and high-resolution, non-marine sequence stratigraphy in avulsion deposits, Cumberland Marshes, Saskatchewan: Sedimentary Geology, v. 139, p. 93–150.

Fielding, C.R., Trueman, J.D., Dickens, G.R., and Page, M., 2003, Anatomy of the buried Burdekin River channel across the Great Barrier Reef shelf: how does a major river operate on a tropical mixed siliciclastic/carbonate margin during sea-level lowstand?: Sedimentary Geology, v. 157, p. 291–301.

Fielding, C.R., Trueman, J.D., and Alexander, J., 2005a, Sedimentology of the modern and Holocene Burdekin River Delta of north Queensland, Australia: controlled by river output, not by waves and tides, *in* Giosan, L., and Bhattacharya, J., eds., River Deltas: Concepts, Models and Examples: SEPM, Special Publication 83, p. 467–496.

Fielding, C.R., Trueman, J.D., and Alexander, J., 2005b, Sharp-based, flood-dominated mouth bar sands from the Burdekin River Delta of northeastern Australia: extending the spectrum of mouth bar facies, geometry, and stacking patterns: Journal of Sedimentary Research, v. 75, p. 55–66.

Fielding, C.R., Trueman, J.D., Dickens, G.R., and Page, M., 2005c, Geomorphology and internal architecture of the ancestral Burdekin River across the Great Barrier Reef shelf, northeast Australia, *in* Blum, M.D., Marriott, S.B., and Leclair, S.F., eds., Fluvial Sedimentology VII: International Association of Sedimentologists, Special Publication 35, p. 321–347.

Galloway, W.E., and Hobday, D.K., 1996. Terrigenous Clastic Depositional Systems: Berlin, Springer-Verlag, Second Edition, 489 p.

Gillespie, R., and Polach, H.A., 1979, The suitability of marine shells for radiocarbon dating of Australian prehistory, *in* Berger, R., and Suess, H., eds., 9th International Conference on Radiocarbon Dating, Proceedings, p. 404–421.

Gomez, B., Carter, L., Trustrum, N.A., Palmer, A.S., and Roberts, A.P., 2004, El Niño-Southern Oscillation signal associated with middle Holocene climate change in intercorrelated terrestrial and marine sediment cores, North Island, New Zealand: Geology, v. 32, p. 653–656.

Goodbred, S.L, Jr, and Kuehl, S.A., 2000, Enormous Ganges–Brahmaputra sediment discharge during strengthened early Holocene monsoon: Geology, v. 28, p. 1083–1086.

Harris, P.T., 1999, Sequence architecture during the Holocene transgression: an example from the Great Barrier Reef shelf, Australia—Comment: Sedimentary Geology, v. 125, p. 235–239.

Harris, P.T., Davies, P.J., and Marshall, J.F., 1990, Late Quaternary sedimentation on the Great Barrier Reef continental shelf and slope east of Townsville, Australia: Marine Geology, v. 94, p. 55–77.

Harvey, R.L., 1998. Geomorphology and sedimentology of abandoned channels on the Burdekin River Delta Plain, northeast Queensland [unpublished Honours Thesis]: Brisbane, University of Queensland, 113 p.

Hesse, P.P., Magee, J.W., and van der Kaars, S., 2004, Late Quaternary climates of the Australian arid region: a review: Quaternary International, v. 118–119, p. 87–102.

Hopley, D., 1970. The geomorphology of the Burdekin Delta, North Queensland: Townsville, Australia, James Cook University of North Queensland, Department of Geography, Monograph Series, 1, 66 p.

Hopley, D., 1972, 1970–1971 research on Quaternary shorelines in Australia and New Zealand—a summary report of the ANZAAS Quaternary Shorelines Committee: Search, v. 3, p. 1–10.

Hopley, D., and Murtha, G.G., 1975. The Quaternary deposits of the Townsville coastal plain, north Queensland, Australia: Townsville, Australia, James Cook University of North Queensland, Department of Geography, Monograph Series, 8, 30 p.

Hori, K., Saito, Y., Zhao, Q.H., and Wang, P.X., 2002, Evolution of the coastal depositional systems of the ChangJiang (Yangtze) River in response to Late Pleistocene–Holocene sea-level changes: Journal of Sedimentary Research, v. 72, p. 884–897.

Johnson, D.P., and Searle, D.E., 1984, Post-glacial stratigraphy, central Great Barrier Reef, Australia: Sedimentology, v. 31, p. 335–352.

Johnson, D.P., Searle, D.E., and Hopley, D., 1982, Positive relief over buried post-glacial channels, Great Barrier Reef province, Australia: Marine Geology, v. 46, p. 149–159.

Jones, B.G., Woodroffe, C.D., and Martin, G.R., 2003, Deltas in the Gulf of Carpentaria, Australia: forms, processes and products, *in* Hasan Sidi, F., Nummedal, D., Imbert, P., Darman, H., and Posamentier, H.W., eds., Tropical Deltas of Southeast Asia—Sedimentology, Stratigraphy, and Petroleum Geology: SEPM, Special Publication 76, p. 21–43.

Kanes, W.H., 1970, Facies and development of the Colorado River Delta in Texas, *in* Morgan, J.P., ed., Deltaic Sedimentation: SEPM, Special Publication 15, p. 78–106.

Kershaw, A.P., 1978, Record of last interglacial-cycle from northeast Queensland: Nature, v. 272, p. 159–161.

Kershaw, A.P., 1983, A Holocene pollen diagram from Lynch's Crater, north-eastern Australia: New Phytologist, v. 94, p. 669–682.

Lang, S.C., Payenberg, T.H.D., Reilly, M.R.W., Hicks, T., Benson, J., and Kassan, J., 2004, Modern analogues for dryland sandy fluvial–lacustrine deltas and terminal splay reservoirs: Australian Petroleum Production and Exploration Association, Journal, v. 44, p. 329–356.

Larcombe, P., and Carter, R.M., 2004, Cyclone pumping, sediment partitioning and the development of the Great Barrier Reef shelf system: a review: Quaternary Science Reviews, v. 23, p. 107–135.
Larcombe, P., Carter, R.M., Dye, J., Gagan, M.K., and Johnson, D.P., 1995, New evidence for episodic post-glacial sea-level rise, central Great Barrier Reef, Australia: Marine Geology, v. 127, p. 1–44.
Leblanc, R.J., 1975, Significant studies of modern and ancient deltaic sediments, *in* Broussard, M.L., ed., Deltas—Models for Exploration: Houston Geological Society, p. 13–85.
Magee, J.W., Miller, G.H., Spooner, N.A., and Questiaux, D., 2004, Continuous 150 k.y. monsoon record from Lake Eyre, Australia: insolation-forcing implications and unexpected Holocene failure: Geology, v. 32, p. 885–888.
Miller, G.H., Mangan, J., Pollard, D., Thompson, S., Felzer, B., and Magee, J., 2005, Sensitivity of the Australian Monsoon to insolation and vegetation: implications for human impact on continental moisture balance: Geology, v. 33, p. 65–68.
Nanson, G.C., Price, D.M., Short, S.A., Young, R.W., and Jones, B.G., 1991, Comparative Uranium–Thorium dating and thermoluminescence dating of weathered Quaternary alluvium in the tropics of northern Australia: Quaternary Research, v. 35, p. 347–366.
Neil, D.T., Orpin, A.R., Ridd, P.V., and Yu, B.F., 2002, Sediment yields and impacts from river catchments to the Great Barrier Reef lagoon: Australian Journal of Marine and Freshwater Research, v. 53, p. 733–752.
Nott, J., and Price, D., 1994, Plunge pools and paleoprecipitation: Geology, v. 22, p. 1047–1050.
Orme, G.R., Webb, J.D., Kelland, N.C., and Sargent, G.E.G., 1978, Aspects of the geological history and structure of the northern Great Barrier Reef: Royal Society (London), Philosophical Transactions, v. A291, p. 23–35.
Orpin, A.R., 1999. Sediment transport, partitioning and unmixing relationships in the mixed terrigenous–carbonate system of the Great Barrier Reef, Burdekin shelf sector, Australia [unpublished Ph.D. Thesis]: Townsville, James Cook University, 73 p.
Orpin, A.R., Ridd, P.V., and Stewart, L.K., 1999, Assessment of the relative importance of major sediment-transport mechanisms in the central Great Barrier Reef lagoon: Australian Journal of Earth Sciences, v. 46, p. 883–896.
Orpin, A.R., Brunskill, G.J., Zagorskis, I., and Woolfe, K.J., 2004, Patterns of mixed siliciclastic–carbonate sedimentation adjacent to a large dry-tropics river on the central Great Barrier Reef shelf, Australia: Australian Journal of Earth Sciences, v. 51, p. 665–683.
Overeem, I., Kroonenberg, S.B., Veldkamp, A., Groenestein, K., Rusakov, G.V., and Svitoch, A.A., 2003, Small-scale stratigraphy in a large ramp delta: recent and Holocene sedimentation in the Volga Delta, Caspian Sea: Sedimentary Geology, v. 159, p. 133–157.
Paine, A.G.L., Gregory, C.M., and Clarke, D.E., 1966, Geology of the Ayr 1:250,000 sheet area, Queensland: Australia, Bureau of Mineral Resources, Geology and Geophysics, Record 1966/88.
Perez-Arlucea, M., and Smith, N.D., 1999, Depositional patterns following the 1870s avulsion of the Saskatchewan River (Cumberland Marshes, Saskatchewan, Canada): Journal of Sedimentary Research, v. 69, p. 62–73.
Postma, G., 1990, Depositional architecture and facies of river and fan deltas: a synthesis, *in* Colella, A., and Prior, D.B., eds., Coarse-Grained Deltas: International Association of Sedimentologists, Special Publication 10, p. 13–27.
Postma, G., 1995, Causes of architectural variations in deltas, *in* Oti, M.N., and Postma, G., eds., Geology of Deltas: Rotterdam, Balkema, p. 3–16.
Pringle, A.W., 2000, Evolution of the east Burdekin Delta coast, Queensland, Australia 1980–1995: Zeitschrift für Geomorphologie, v. 44, p. 273–304.
Reading, H.G., and Collinson, J.D., 1996, Clastic Coasts, *in* Reading, H.G., ed., Sedimentary Environments: Processes, Facies and Stratigraphy, Third Edition: Oxford, U.K., Blackwell Science, p. 154–231.
Rodriguez, A.B., Hamilton, M.D., and Anderson, J.B., 2000, Facies and evolution of the modern Brazos Delta, Texas: wave versus flood influence: Journal of Sedimentary Research, v. 70, p. 283–295.
Searle, D.E., 1983, Late Quaternary regional controls on the development of the Great Barrier Reef—geophysical evidence: Bureau of Mineral Resources, Journal of Australian Geology and Geophysics, v. 8, p. 267–276.
Shulmeister, J., 1992, A Holocene pollen record from lowland tropical Australia: The Holocene, v. 2, p. 107–116.
Stouthamer, E., and Berendsen, H.J.A., 2001, Avulsion frequency, avulsion duration, and interavulsion period of Holocene channel belts in the Rhine–Meuse delta, The Netherlands: Journal of Sedimentary Research, v. 71, p. 589–598.
Ta, T.K.O., Nguyen, V.L., Tateishi, M., Kobayashi, I., Saito, Y., and Nakamura, T., 2002, Sediment facies and late Holocene progradation of the Mekong River Delta in Bentre Province, southern Vietnam: an example of evolution from a tide-dominated to a tide- and wave-dominated delta: Sedimentary Geology, v. 152, p. 313–325.
Thom, B.G., Hails, J.R., Martin, J.R.H., and Phipps, C.V.G., 1969, Radiocarbon evidence against post-glacial sea levels in eastern Australia: Marine Geology, v. 7, p. 161–168.
Törnqvist, T.E., 1994, Middle and late Holocene avulsion history of the River Rhine (Rhine–Meuse delta, Netherlands): Geology, v. 22, p. 711–714.
Trueman, J.D., 2002. Stratigraphy and sedimentology of the Burdekin Delta, Queensland, and comparisons with Permian coastal facies in the Denison Trough, SW Bowen Basin, Australia [unpublished Ph.D. Thesis]: Brisbane, University of Queensland, 256 p.
Tye, R.S., and Coleman, J.M., 1989, Depositional processes and stratigraphy of fluvially dominated lacustrine deltas, Mississippi Delta Plain: Journal of Sedimentary Petrology, v. 59, p. 973–996.
Van Wagoner, J.C., Mitchum, R.M., Jr, Campion, K.M., and Rahmanian, V.D., 1990, Siliciclastic Sequence Stratigraphy in Well Logs, Core and Outcrops: Concepts for High-Resolution Correlation of Time and Facies: American Association of Petroleum Geologists, Methods in Exploration Series, v. 7, 55 p.
Way, A.J., 1987. Post-glacial stratigraphy of Upstart Bay, off the Burdekin River, north Queensland [unpublished M.Sc. Thesis]: Townsville, James Cook University, 149 p.
Woolfe, K.J., Larcombe, P., Naish, T., and Purdon, R.G., 1998, Lowstand rivers need not incise the shelf: an example from the Great Barrier Reef, Australia, with implications for sequence stratigraphic models: Geology, v. 26, p. 75–78.
Wright, L.D., 1977, Sediment transport and deposition at river mouths: a synthesis: Geological Society of America, Bulletin, v. 88, p. 857–868.
Wyrwoll, K.-H., and Miller, G.H., 2001, Initiation of the Australian summer monsoon 14,000 years ago: Quaternary International, v. 83–85, p. 119–128.

Received 24 April 2005; accepted 6 October 2005.